Title: The glymphatic system clears amyloid beta and tau from brain to plasma in humans

Authors: Jeffrey J. Iliff, PhD[1,2,3]; Donald L. Elbert, PhD[3]; Laurent Giovangrandi, PhD[4]; Tarandeep Singh, MS[4]; Venky V. Venkatesh, PhD, PMP[5]; Alejandro Corbellini, PhD[4]; Robert M. Kaplan, PhD[6]; Elizabeth Ludington[7], PhD; Kevin Yarasheski, PhD[5]; Jeffrey Lowenkron[8], MD, MPP; Carla VandeWeerd, PhD[9,10]; Miranda M. Lim, MD, PhD[11,12,13]; Paul Dagum, MD, PhD[4]

Affiliations:[1]VISN 20 Northwest Mental Illness Research, Education and Clinical Center, VA Puget Sound Healthcare System, Seattle WA; [2]Department of Psychiatry and Behavioral Sciences; [3]Department of Neurology, University of Washington School of Medicine, Seattle WA; [4]Applied Cognition Inc., Redwood City CA; [5]C_2N Diagnostics, St. Louis, MO; [6]Clinical Excellence Research Center, Stanford University School of Medicine, Stanford, CA; [7]Epalla Consulting, San Diego, CA; [8]The Villages Health System, The Villages, FL; [9]University of Florida Precision Health Research Center, University of Florida, Gainesville, FL; [10]Health Outcomes and Biomedical Informatics, College of Medicine, University of Florida, Gainesville, FL; [11]VISN 20 Northwest Mental Illness Research, Education and Clinical Center (MIRECC), VA Portland Health Care System, Portland, OR; [12]Neurology Service, Research Service, VA Portland Health Care System, Portland, OR; [13]Department of Neurology, Oregon Alzheimer's Disease Research Center, Oregon Health & Science University, Portland, OR

Corresponding Author:
Paul Dagum, MD PhD
Applied Cognition Inc
1629 Main St.
Redwood City, CA 94063
paul@appliedcognition.com
Ph: (415) 378-5456

ABSTRACT

Poor sleep is implicated in the development of Alzheimer's disease (AD) pathology and cognitive impairment. The glymphatic system has been proposed as a link between sleep disruption and AD, and in animal models glymphatic impairment is sufficient to drive the development of AD pathology. It remains unknown whether the glymphatic system clears amyloid beta (Aβ) and tau from the brain in humans. In a multi-site randomized crossover clinical trial (N=39), participants underwent overnight in-laboratory conditions of normal sleep and sleep deprivation following instrumentation that included a novel device to measure brain parenchymal resistance to glymphatic flow (R_P) by transcranial multifrequency impedance spectroscopy and sleep electroencephalography (EEG). This study directly tested the hypothesis that sleep-active glymphatic clearance increases morning plasma AD biomarker levels. The primary outcomes were the change in plasma levels of AD biomarkers (Aβ40, Aβ42, np-tau181, np-tau217 and p-tau181) from evening to morning predicted by R_P, sleep EEG features, and heart rate. We found that changes in R_P, heart rate and EEG delta power predicted changes in Aβ42 ($p<0.001$), np-tau181 ($p=0.002$), np-tau217 ($p<0.001$) and p-tau181 ($p<0.001$). The predicted changes replicated those from a multicompartment model based on published data on Aβ and tau efflux from brain to plasma. Our findings show that elements of sleep-active physiology, in particular decreased brain parenchymal resistance, facilitates the clearance of AD biomarkers to plasma, supporting a role for glymphatic clearance in these processes, and suggesting the enhancement of glymphatic function as a therapeutic target to reduce the development and progression of AD pathology in at-risk populations.

KEYWORDS

glymphatic, sleep, Alzheimer's, amyloid beta, tau, plasma, clearance, morning plasma

INTRODUCTION

Sleep disruption is associated with increased risk of Alzheimer's disease (AD) in epidemiological studies[1-3], while biomarker studies in cognitively-intact participants suggest that short sleep duration and poor sleep quality are associated with greater AD-related amyloid β (Aβ) and tau pathology[4-9], even before the onset of clinical symptoms of cognitive and functional decline. Yet the mechanistic link between sleep disruption and AD risk remains undefined. The glymphatic system is a brain-wide network of perivascular pathways along which cerebrospinal fluid (CSF) and interstitial fluid (ISF) exchange, supporting the clearance of interstitial solutes from the brain into the CSF, and thence into the blood. Studies in mice demonstrated that glymphatic function contributes to the clearance of Aβ and tau, is more rapid during sleep, and is impaired by acute sleep deprivation[10-13]. While more rapid glymphatic clearance of solutes during sleep has now been validated in the human brain[14,15], no study has tested mechanistically whether sleep-active glymphatic activity contributes to the clearance of Aβ and tau in a healthy human population.

Plasma biomarkers have emerged as a potentially critical tool enabling the non-invasive diagnosis of AD at a large scale within the wider population. Immuno-assay and mass spectrometry-based measures of different Aβ and tau species permit the assessment of AD-related Aβ plaque burden and tau pathology, even during preclinical stages of disease in the years prior to patients' clinical progression to cognitive impairment and dementia[16,17]. Although generally regarded as steady-state indicators of brain AD pathological burden, plasma AD biomarker levels are impacted acutely by sleep disruption[4,18]. In a crossover study including 5 healthy participants, plasma $A\beta_{40}$, $A\beta_{42}$, non-phosphorylated tau181 (np-tau181), non-phosphorylated tau217 (np-tau217) and phosphorylated tau181 (p-tau181) were each reduced during the overnight period by acute sleep deprivation[4]. Noting an increased ratio of

CSF:plasma Aβ and tau levels, the authors inferred that the processes governing the clearance of Aβ and tau from the brain to the CSF, and then from the CSF to the plasma must be impaired by acute sleep deprivation. These findings are consistent with the sleep-active glymphatic clearance of Aβ and tau from the brain, yet they do not provide causal support.

Here we deigned a study to directly test if sleep-active glymphatic function contributes to the overnight clearance of Aβ and tau from the human brain. We first developed a compartmental pharmacokinetic model to predict the effect that sleep-active glymphatic transport between the brain ISF and CSF would have on morning plasma levels of Aβ and tau species. We then carried out a clinical randomized crossover study where participants underwent overnight normal sleep and sleep deprivation. Prior studies in rodents and humans demonstrate that glymphatic function increases with increasing sleep electroencephalography (EEG) delta power, reduced EEG beta power, reduced heart rate (HR), and reduced brain parenchymal resistance to fluid flow (R_P)[13,19-21]. Measuring these key determinants of glymphatic exchange by sleep EEG and impedance spectroscopy with a novel investigational device[21], we defined the relationship between sleep features, R_P, and HR and changes in morning and evening plasma AD biomarker levels. Using this approach, we directly tested the hypothesis that sleep-active glymphatic clearance increases morning plasma AD biomarker levels.

RESULTS

Compartmental pharmacokinetic model relating glymphatic exchange to plasma AD biomarker levels

To understand the effect that sleep-active glymphatic clearance has on plasma AD biomarker levels, we developed a 4-compartment model of solute transport and elimination from the brain ISF (**Figure 1A**). This is a simplification of prior models[22], and includes the free ISF (**1**), CSF (**2**),

plasma (**3**) and neuropil (**4**) compartments. Degradation within the neuropil, and peripheral clearance from the plasma are also represented in the model. Solute transport processes and their rate constants for Aβ and tau species based on literature values[22] are provided in **Table 1**.

This model was solved under two different conditions. Under the **null model**, the transport of solutes between the ISF Free compartment (**1**) and the Plasma (**3**) compartment was defined under conditions in which sleep-active glymphatic exchange did not occur, reflected in the rate constants k_{12} and k_{21} between ISF (**1**) and CSF (**2**) remaining invariant across sleep and waking (or sleep deprivation) conditions. Under the **glymphatic model**, k_{12} and k_{21} increased with sleep, reflecting the sleep-active CSF solute influx and interstitial solute efflux reported in rodents and humans[13,15].

Using first-order kinetics and published rate constants (**Table 1**), the time-dependent release of an arbitrary unit of Aβ and tau into the brain ISF and the resulting plasma concentrations of Aβ and tau were modeled over 24 hours under (a) the **null model** with time-invariant k_{12} and k_{21} and (b) the **glymphatic model** in which k_{12} and k_{21} were allowed to increase. A full derivation and solution for these models is provided in **Supplemental Methods and Results**. **Figure 1B** (top) depicts the resulting compartmental concentrations of Aβ and tau over 24 hours following their release into the ISF at time $t = 0$ under the **null model** (solid lines) and **glymphatic model** (dashed lines). Dotted lines show the model outputs when CSF-ISF exchange is reduced during the overnight period. **Figure 1B** (bottom) shows Aβ and tau concentrations only within the plasma compartment. Within this model, both Aβ and tau concentrations in the plasma increase in the **glymphatic model** compared to the **null model** over the entire 24 hr period. Furthermore, as detailed in **Supplementary Methods and Results**, a linear approximation of these models in the domain of interest demonstrates that under the **null model**, morning

plasma Aβ and tau concentrations would be linearly dependent upon evening plasma levels only, while under the **glymphatic model**, morning plasma Aβ and tau concentrations would be related to an interaction term between the evening plasma levels and the variable rate constants k_{21} and k_{12} .

These results provide two concrete predictions that permit us to test the hypothesis that sleep-active glymphatic exchange contributes to overnight changes in plasma AD biomarker levels. Under the **glymphatic model**, **1)** overnight sleep deprivation would reduce morning plasma AD biomarker levels compared to those following normal sleep; **2)** under conditions of sleep deprivation, morning plasma AD biomarker levels would be linearly dependent upon evening biomarker levels alone, while under normal sleep conditions morning plasma AD biomarker levels will be increased by the interaction term between evening plasma levels and features of sleep-active glymphatic function contributing to greater clearance.

Clinical study design, inclusion and exclusion criteria

As described previously[21], we conducted two cross-over clinical studies in which participants underwent one night of normal sleep and one night of sleep deprivation, in randomized order and separated by two or more weeks (**Figure 2A**). One study was conducted in The Villages® community in Central Florida where the University of Florida maintains a satellite academic research center, The UF Health Precision Health Research Center (UF Health PHRC). The second study was carried out at the University of Washington (UW) in Seattle. Study participants underwent peripheral blood draws at 1900 hrs and 0700 hrs, prior to and following the overnight sleep and sleep deprivation periods. Plasma AD biomarkers, including $A\beta_{40}$, $A\beta_{42}$, np-tau181, np-tau217, p-tau181, and phosphorylated tau217 (p-tau217) were quantified using C_2N Diagnostics' immunoprecipitation liquid chromatography-tandem mass spectrometry

platforms[23-26]. During the overnight period, participants were instrumented with an investigational in-ear wearable device that measured key determinants of glymphatic function, including sleep features hypnogram and spectral band power by electroencephalography (EEG), heart rate (HR) by photoplethysmography (PPG), and brain parenchymal resistance (R_P) by dynamic impedance spectroscopy (**Figure 2B**). A detailed description of this device, the validation of its sleep EEG measures against gold-standard overnight polysomnography, and of the measures of R_P against contrast-enhanced magnetic resonance imaging (CE-MRI)-based measures of glymphatic function has recently been reported[21].

All studies were performed between October 2022 – June 2023 and were reviewed and approved by University of Florida Institutional Review Board (IRB No. 202201364, Villages study) and Western Institutional Review Board (IRB No. 20225818, UW study). The studies have been registered at ClinicalTrials.gov (https://clinicaltrials.gov/study/NCT06060054 and https://clinicaltrials.gov/study/NCT06222385). Written informed consent was obtained from all study participants during a screening visit, prior to any study activities. Studies were carried out in accordance with the principles of the Belmont Report. The Villages Study enrolled 34 healthy participants 56-66 years of age. The UW Study enrolled 14 healthy participants 49-63 years of age. Participants were excluded if they had cognitive impairment or clinical depression. Cognitive impairment was assessed using the Montreal Cognitive Assessment (MoCA, 28.1 +/- 1.2; range 26, 30) and depression was evaluated using the 15-item Geriatric Depression Scale (GDS, 0.7 +/- 1.1; range 0, 4). Participants with a self-reported history of diabetes, hypertension, coronary artery disease, pulmonary disease, neurological disease, depression or anxiety were also excluded from the study, as were participants planning travel to alternate time zones within two weeks of study participation. Participant demographics, MoCA and GDS scores are listed for each study site and for the combined dataset in **Table 2**.

A Consolidated Standards of Reporting Trials (CONSORT) diagram for the Villages Study and UW Study is provided in **Figure 2C.** Within the Villages Study, the first three participants were removed from analysis because of a sensor position change in the investigational device. One participant was unable to complete the first MRI session and withdrew from the study. Of the remaining 30 participants (61.8 ± 2.7 years of age; 14 female, 16 male) that completed the Villages Study, five overnight sleep studies and eight overnight wake studies failed data quality control due to excessive artifacts in the recordings, leaving 25 sleep studies and 22 wake studies with analyzable device and biomarker data in the Villages Study. Of the participants enrolled in the UW Study, one was not compliant with the enforced wake protocol and was removed from analysis. The remaining 14 participants (55.6 ± 4.6 years of age; 7 female, 7 male) all completed the protocol. All overnight sleep data were usable, but two overnight wake studies were removed because of excessive artifact in the UW Study.

Developing a multivariate model to relate multiple sleep-related glymphatic features to Aβ and tau clearance to the plasma

Studies in rodents and humans have shown that glymphatic function is increased with increasing EEG delta band power, reduced EEG beta band power, and reduced HR[19-21]. Glymphatic function during sleep is more rapid with increased brain extracellular volume fraction as observed in rodents[13], reflected in reduced R_P during sleep in human participants[21]. Changes in ventricular CSF dynamics and low-frequency brain pulsations believed to reflect glymphatic function have been linked to specific sleep stages and their associated features[27,28]. Thus, several sleep-related features, including hypnographic sleep stages, sleep EEG spectral bands, HR and R_P, which all track with glymphatic function were captured for each participant in the present study. In rodent models, glymphatic function has been implicated in the clearance of both Aβ and tau[10,13,29-31]. In the present study, we measured several different plasma Aβ

($A\beta_{40}$, $A\beta_{42}$) and tau species (np-tau181, np-tau217, p-tau181, p-tau217) at evening and morning timepoints in each participant following overnight of sleep and sleep deprivation (**Table 3**). The measured plasma levels and overnight changes with sleep agree with prior reported values for $A\beta_{40}$, $A\beta_{42}$ and p-tau181[32].

We developed a series of multivariate mixed models to define the effects that overnight continuous features of glymphatic physiology have on overnight clearance of brain interstitial Aβ and tau to the plasma. Within these models, the multiple dependent variable measures for each participant were the morning plasma Aβ and tau ($A\beta_{40}$, $A\beta_{42}$, np-tau181, np-tau217, p-tau181) biomarker levels. Plasma p-tau217 levels were measured but excluded from analysis because a large proportion (9 out of 49) of these cognitively-intact individuals exhibited plasma p-tau217 levels below the limit of detection for the assay, consistent with prior study findings[33,34]. Within these models, two separate groups of predictors were analyzed focusing alternatively on EEG spectral features (***Power***) and hypnographic sleep stages (***Hypno***). Separating the predictors into these two groups avoided multicollinearity in the regression models as previously documented[21]. The first group included EEG delta and beta power bands, parenchymal resistance R_P, and HR. The second was comprised of hypnographic sleep stages, including rapid eye movement (REM), N2 and N3 non-REM (NREM), total sleep time (TST), R_P, and HR. In order to capture the important effect that the interactions between the predictors and evening plasma Aβ and tau biomarkers had on morning plasma Aβ and tau, we used dimensionality reducing single-index regression[35]. Each group of predictors was combined using linear combinations into three single-index predictors: EEG power band predictors under the sleeping condition (***Power***$_S$) and under the sleep deprivation/wake condition (***Power***$_W$), and sleep hypnogram predictors under the sleeping condition (***Hypno***$_S$). The single-index regression selection of included predictors and choice of weights from each group into the linear

combinations used optimization to find the single linear combination of the regressor predictors that minimized the Akaike Information Criterion (AIC) of the multivariate mixed models and are described in detail within **Supplementary Methods and Results.** The optimal predictor components and weights for the sleep condition (***Power$_S$, Hypno$_S$***) and sleep deprivation/wake condition (***Power$_W$***), where the sum of the squared weights normalizes to unity, are provided in **Table 4.**

Parallel multivariate linear mixed models representing the **null model** and the **glymphatic model** were developed, as described in detail in **Supplemental Methods and Results.** Under the **null model**, morning plasma levels of Aβ and tau species were not dependent upon sleep-active glymphatic exchange, and thus were not assumed to be influenced by EEG spectral (***Power***) and hypnogram sleep stage (***Hypno***) predictors. Rather the morning plasma levels of AD biomarkers (***Conc$_{AM}$***) were regressed on the evening plasma AD biomarker levels (***Conc$_{PM}$***) for Aβ and tau biomarkers ($A\beta_{40}$, $A\beta_{42}$, np-tau181, np-tau217, p-tau181), and an indicator variable denoting participant amyloid-positive status using the $A\beta_{42}/A\beta_{40} < 0.089$ cutoff[24,26,36]. Potentially confounding variables age, sex, APOE-ε4 status, and study site were included in the model. These multivariate mixed models used participant ID as a random intercept. The **glymphatic model** shares the features of the **null model**, with the addition that morning plasma AD biomarker levels were dependent upon increased overnight ISF-CSF exchange. Thus, the **glymphatic model** included the direct effect of evening plasma AD biomarker levels (***Conc$_{PM}$***) upon morning levels (***Conc$_{AM}$***), but also included the effects of the ***Power$_S$***, ***Power$_W$*** and ***Hypno$_S$*** predictors, and their respective interaction terms with evening levels of plasma AD biomarkers (***Power$_S$ * Conc$_{PM}$***, ***Hypno$_S$ * Conc$_{PM}$***, ***Power$_W$ * Conc$_{PM}$***). The likelihood ratio test (LRT) of the **glymphatic model** versus the **null model** was used to determine which model

performed better at predicting the morning plasma Aβ and tau biomarker levels. This is described in detail in **Supplementary Methods and Results.**

Lower parenchymal resistance and higher EEG delta power during sleep increase overnight clearance of Aβ and tau to the plasma

We first evaluated EEG spectral features, HR and R_P as predictors of changes in plasma AD biomarker levels occurring during overnight sleep. The predictor ***Power*$_S$** that led to the best fit of the data based on the AIC for the **glymphatic model** in sleep included only R_P and EEG delta power, and not EEG beta power or HR (**Table 4**). In this case, R_P was the overwhelming contributor to ***Power*$_S$**. The output of the **null model** and **glymphatic model** with the predictor ***Power*$_S$** are shown in **Table 5**. Estimates for single predictor coefficients within the **glymphatic model** for each plasma AD biomarker are provided in **Table 6**.

By including overnight R_P and EEG delta power in the single predictor ***Power*$_S$**, the **glymphatic model** led to greater predictive performance over the **null model** (**Table 7**, LRT, $p < 0.001$). When comparing the percent variance of morning plasma AD biomarker levels that was explained by including overnight R_P and EEG delta power in the **glymphatic model** and that was not explained by the **null model**, the **glymphatic model** explained between 23.7% (np-tau217) to 48.4% ($A\beta_{40}$) of that variance (**Table 8**).

The compartmental pharmacokinetic model predicts that sleep-active glymphatic function will increase morning plasma AD biomarker levels (**Figure 1A-B**). Consistent with this prediction, as shown in **Tables 4-5** and, at the mean value of each evening plasma AD biomarker level, a decrease in overnight sleep ***Power*$_S$**, corresponding to decreased brain parenchymal resistance R_p and increased in EEG delta power, led to an increase in morning plasma AD biomarker

levels for each species, except $A\beta_{40}$ which did not achieve statistical significance. This suggests that decreased parenchymal resistance R_P and increased EEG delta power during sleep, both of which are associated with greater glymphatic exchange in rodents and humans[13,19,21], supported the clearance of brain interstitial Aβ and tau to the plasma. These features also explain approximately one-third of the unexplained variance in morning plasma levels arising from the **null model** by itself (**Table 8**).

Lower heart rate and parenchymal resistance, but not differences in overnight sleep stages, increase clearance of Aβ and tau to the plasma

We next tested whether differences in overnight sleep stages influenced the clearance of Aβ and tau to the plasma. The predictor ***Hypno$_S$*** was constructed from all possible subsets of regressors chosen from EEG hypnogram stages (N2, N3, REM), TST, HR and R_p that led to the best fit of the data based on the AIC for the **glymphatic model** in sleep, and included N2 time, REM time, HR and R_p, although only the contributions of HR and R_P were significant (**Table 4**). The **null model** and the **glymphatic model** fitted to the morning plasma AD biomarker level data following overnight sleep with the ***Hypno$_S$*** predictor are shown in **Table 9**. By including overnight N2 time, REM time, R_P and HR in the single predictor ***Hypno$_S$***, the **glymphatic model** led to greater predictive performance over the **null model** (**Table 7**, LRT, $p < 0.001$). When comparing the percent variance of post-sleep morning plasma AD biomarker levels that was explained by including overnight R_p and HR in the **glymphatic model** and that was not explained by the **null model**, the **glymphatic model** explained between 37.1% (np-tau217) to 66.8% (Aβ40) of that variance (**Table 8**).

Under the **glymphatic model** where Aβ and tau exchange between the ISF and CSF compartments increases during sleep, the multicompartment simulation predicted that sleep-

active glymphatic exchange would increase morning plasma AD biomarker levels. **Table 6** and **Table 9** show that at the mean value of each evening plasma AD biomarker level, a decrease in overnight ***Hypno$_S$***, which corresponds to a decrease in both R_P and HR, increases morning plasma biomarker levels for all Aβ and tau species. These findings suggest that reduced brain parenchymal resistance R_P and HR, which are associated with increased glymphatic function in rodents[13,19] and humans[21], increases the clearance of ISF Aβ and tau to the plasma. These effects explain approximately one-half of the unexplained variance in the morning plasma AD biomarker levels from the **null model** (**Table 8**).

Higher EEG delta and beta power, and higher heart rate reduce Aβ and tau clearance to the plasma during overnight sleep deprivation

We last evaluated whether EEG spectral features, HR or R_P influenced AD biomarker clearance to the plasma under conditions of overnight sleep deprivation/waking. In contrast to the prior sleep condition **glymphatic models**, the sleep deprivation/wake **glymphatic model** behaved in a markedly different manner. In this **glymphatic model**, the predictor ***Power$_W$*** that was constructed from all possible subsets of regressors chosen from EEG power bands, HR and R_p to best fit the sleep deprivation data included delta power, beta power and HR, but not R_p (**Table 4**). Interestingly, the sign of the EEG delta power component in the ***Power$_W$*** model was opposite to its sign in the ***Power$_S$*** for the **glymphatic model**. The **null model** and **glymphatic model** fitted to the morning plasma AD biomarker levels following overnight sleep deprivation using the ***Power$_W$*** predictor are shown in **Table 10**. By including overnight EEG delta power, EEG beta power and HR in the single predictor ***Power$_W$***, the sleep deprivation **glymphatic model** led to greater predictive performance of morning plasma AD biomarker levels over the **null model** (**Table 7**, LRT, $p < 0.001$). However, when comparing the percent variance of morning plasma biomarker levels that was explained by including sleep deprivation EEG delta

power, EEG beta power and HR in the **glymphatic model** but that was not explained by the **null model**, the sleep deprivation **glymphatic model** failed to reduce the variance on any of the biomarkers (**Table 8**).

*The predictors **Power$_S$**, **Hypno$_S$** and **Power$_W$** in the glymphatic model replicate the rate constants in the compartment model for glymphatic clearance of amyloid β and tau*

The linear interaction terms between the predictors ***Power$_S$***, ***Hypno$_S$*** and ***Power$_W$*** and evening plasma AD biomarker levels in the three **glymphatic models** where significant at both the group level (**Table 11**) and individual levels (**Tables 4, 8 and 9**). These interaction terms are the same as described by **Equation 3** in the solution of the multi-compartment model (**Supplementary Methods and Results**). That is, the linear interaction terms between the predictors ***Power$_S$***, ***Hypno$_S$*** and ***Power$_W$*** and evening plasma AD biomarker levels are consistent with multicompartment first-order kinetics under the **glymphatic model** assumption with ISF to CSF clearance rate constants that are time-varying through ***Power$_S$***, ***Hypno$_S$*** and ***Power$_W$***. To further demonstrate this correspondence, we compared the predictions of morning plasma AD biomarker levels when ***Power$_S$***, ***Hypno$_S$*** and ***Power$_W$*** were varied to the predictions made by the compartment model by varying the rate constants k_{21} and k_{12}. As shown in **Figure 3A-C**, we observed that when we vary the magnitude of the fitted predictors in the **glymphatic models** and the rate constants k_{21} and k_{12} in the compartment model by the same amount, the change in glymphatic clearance of AD biomarker to blood predicted by both models is similar. It is noteworthy that while the results of the statistical and compartmental models converge, they were derived from independent sources. The glymphatic models were statistically estimated from the data of the Villages and UW Studies whereas the compartment model was based on the elimination kinetics of amyloid β and tau obtained from independent published research[22].

DISCUSSION

We developed a compartmental transport model based on published kinetic values to predict the effect that sleep-active glymphatic CSF-ISF exchange would have on overnight changes in plasma AD biomarker levels. We then conducted a rigorous test of the glymphatic model of interstitial Aβ and tau clearance from the human brain during sleep with a multi-site randomized cross-over clinical study design, which used a novel investigational device from Applied Cognition[21] to measure glymphatic flow resistance R_P, sleep EEG features, and HR, and clinically validated blood-based biomarkers of Aβ and tau provided by C_2N[24] in healthy older participants undergoing both overnight sleep and sleep deprivation visits. These studies demonstrated that reduced R_P, increased EEG delta power, and reduced HR were associated with higher morning levels of plasma Aβ and tau. The inclusion of these predictors of sleep-active glymphatic clearance explained between 30-70% of the residual variance in morning plasma AD biomarker levels not explained by the model that did not include these predictors and assumed overnight CSF-ISF exchange was constant. Sensitivity analysis of the compartmental model derived from published literature transport values, and the statistical model which was derived from these clinical experimental data, showed that the results from the independent approaches converged across a wide range of input values. These findings support a key role for the sleep-active glymphatic clearance of Aβ and tau from the brain, reflected in overnight changes in plasma AD biomarker levels.

The burden of Aβ and phosphorylated tau in the brain is diagnostic for AD and prognostic of its progression[37-39]. Recently approved monoclonal antibody therapies targeting Aβ demonstrate marked reduction in brain Aβ burden, but at present provides only modest improvement in cognitive outcomes and quality of life[40,41]. This apparent shortcoming has led to an increasing interest in extending anti-Aβ immunotherapy into earlier, preclinical stages of AD and into at-risk

populations such as *APOE-ε4* carriers. It is also possible that if the mechanisms contributing to the development and progression of Aβ and tau pathology can be defined, then it may be possible both to better identify individuals at risk of the development of this pathology and to intervene in at-risk individuals to prevent its development and eventual progression.

In rodent models, sleep-active glymphatic function has been implicated in the clearance of both Aβ and tau. Interstitial Aβ and tau both move through brain tissue along perivascular pathways[10,29], while inhibition of glymphatic function by either *Aqp4* or *Snta1* gene deletion slows the clearance of Aβ and tau and promotes the development of Aβ and tau pathology[10,13,29-31,42-45]. Glymphatic function is impaired in animal models of aging[46], cerebrovascular dysfunction[47,48], traumatic brain injury[29,49-51], and sleep disruption[13,52]; each of which are non-genetic risk factors for Alzheimer's disease. This body of results from rodent studies suggests that impairment of glymphatic clearance of Aβ and tau is a key factor in the development of AD, serving as a mechanistic linkage between a wide spectrum non-genetic AD risk factors and the development of AD-related Aβ and tau pathology[53]. If true, then the detection of glymphatic impairment would permit the identification of individuals at risk for the development of Aβ and tau pathology, while targeting glymphatic function would provide a novel approach to the prevention of the development and progression of AD pathology in at-risk individuals.

Despite promising results from rodent studies, key biological features of sleep-active glymphatic function have only recently been confirmed in the human brain. Intrathecal contrast-enhanced MRI studies have demonstrated extensive CSF-ISF exchange in the human brain[14], that this exchange is organized along the axis of the cerebral arterial vasculature[54], and that ISF solute clearance is more rapid in the sleeping compared to the waking brian[15]. In a recent study, we

demonstrated that glymphatic function is sleep-active, and enhanced during sleep by increasing EEG delta power, reduced EEG beta power, reduced HR, and reduced parenchymal resistance R_P[21]. Yet while a recent study[4] suggested that the CSF-to-blood clearance of Aβ and tau are impaired by acute sleep deprivation, no study has yet demonstrated that sleep-active glymphatic exchange contributes to the clearance of Aβ and tau from the human brain.

To test whether sleep-active glymphatic function contributes to the clearance of Aβ and tau from the human brain, we first developed a multicompartment model of Aβ and tau clearance from the brain interstitium to predict the effects that sleep-related changes in glymphatic CSF-ISF exchange would have on evening-to-morning changes in AD biomarker levels. The change in glymphatic clearance was modeled as a change in the rate constants between ISF and CSF compartments and showed that an overnight increase in exchange should lead to higher plasma AD biomarker levels the next morning.

Analyzing data from two cross-over design clinical studies, we evaluated the validity of two parallel models to explain overnight changes in plasma AD biomarker levels. Our null hypothesis was that glymphatic flow made no contribution to the overnight clearance of AD plasma biomarkers, and the null model used only the evening AD plasma biomarker levels adjusted by biological confounders to predict the morning AD biomarker levels. The null model explained 62%-98% of the variance in the morning AD plasma biomarker levels in the sleep condition, but only 32%-77% in the sleep deprivation/awake condition. This explained variance was dominated by within-individual effects, and was statistically accommodated in the random intercepts model that utilized participant as a random effect. The glymphatic hypothesis was that increased CSF-ISF exchange during sleep increased the overnight clearance of Aβ and tau from brain to the plasma. Because glymphatic function during sleep is regulated by increased

EEG delta power, reduced EEG beta power and HR, and reduced R_P[13,19,21], we tested if the inclusion of these features would improve the prediction of AD plasma biomarker levels consistent with our multicompartment model prediction. Using a single-index regression that linearly combined these variables into single predictors ***Power$_S$*** for sleep and ***Power$_W$*** for wake, the glymphatic model was able to explain 30%-48% of the residual morning AD plasma biomarker variance during the sleep condition but *none* of the residual morning variance for the wake condition. The optimal predictor ***Power$_S$*** that minimized the AIC in the sleep condition was dominated by R_P with a small contribution from EEG delta power. In contrast, the optimal predictor for the wake condition did not include R_P and was a mix of EEG delta power, beta power and HR. When we tested the glymphatic hypothesis using a single-index predictor for the sleep condition constructed from sleep stage duration, HR and glymphatic flow resistance, the predictor was again primarily glymphatic flow resistance R_P with some contribution from HR. This latter model was able to explain from 37%-67% of the residual morning AD plasma biomarker variance in the sleep condition.

While it is widely appreciated that glymphatic clearance is more rapid during sleep than during waking, glymphatic clearance does occur during wake[13,15,21]. Yet to what extent this clearance is modifiable by sleep-like physiology during waking is unknown. The wake prediction model using ***Power$_W$*** was notable in that only the non-phosphorylated tau emerged as significant, which also agreed with the multicompartment model predictions for tau in wake. Sleep deprivation has been shown to increase non-phosphorylated tau levels, assumed to be from increased neuronal activity leading to greater non-phosphorylated tau release into the ISF[55,56]. The optimal single predictor ***Power$_W$***, however, showed that contributions from EEG delta power, beta power and HR having lower values resulted in higher morning AD biomarker levels. This finding suggests that in the context of higher non-phosphorylated tau release during sleep deprivation from higher neuronal activity, clearance remains modifiable with lower beta power and HR increasing

clearance similar to their effect in sleep[13,15,19,21]. The relationship with increased EEG delta power and reduced clearance during sleep deprivation appears at first glance, to be contradictory. It is important to note that while during sleep, deep N3 slow wave sleep is associated with higher delta band power, during waking and sleep deprivation, increasing delta band power reflects the accumulation of sleep pressure[57], potentially explaining the relationship between higher sleep deprivation EEG delta power and reduced morning plasma AD biomarker levels.

The absence of a contribution to $\boldsymbol{Power_W}$ from brain parenchymal resistance R_p is also notable. While this might suggest that brain extracellular volume fraction remains stable during sleep deprivation or during waking, the "runner up" best fit predictor to $\boldsymbol{Power_W}$ did include R_p with EEG delta power, EEG beta power and HR. The respective weights were 0.244, 0.355, 0.304 and 0.850. Between the best fit predictor $\boldsymbol{Power_W}$ and this "runner up" $\boldsymbol{Power_W}$, the weights to EEG delta power, EEG beta power and HR were similar, while the weight or contribution of R_P is substantially smaller than its contribution to the best fit predictors $\boldsymbol{Power_S}$ and $\boldsymbol{Hypno_S}$. This "runner up" best fit predictor $\boldsymbol{Power_W}$ optimized the maximum likelihood of the data, had an AIC that differed by less than 1 from the best fit predictor $\boldsymbol{Power_W}$ and would be considered an equivalent model under the AIC test[58]. Under this predictor, an increase in parenchymal resistance R_P would also contribute to a decrease in morning plasma AD biomarker levels.

We were further able to show from these data that a simulated change in the glymphatic model $\boldsymbol{Power_S}$ or $\boldsymbol{Hypno_S}$ single-index predictors led to predicted changes in AD biomarker clearance to plasma that replicated the predictions made by the multicompartment model when similar magnitude changes were made to the CSF-ISF rate constants. Considering that the multicompartment model was derived from external published data[22], this finding independently corroborates the findings from our experimental data and statistical model. Together these

results affirm the glymphatic hypothesis, that increased CSF-ISF exchange during sleep supports the overnight clearance of Aβ and tau from the human brain.

In addition to supporting a role for glymphatic flow in the clearance of Aβ and tau, the present results provide additional mechanistic insights into how these processes unfold in the human brain. Consistent with prior studies in rodents[19,20] and humans[21], EEG delta power during sleep contributed to increasing clearance of Aβ and tau to the plasma in the overnight period. Surprisingly, while sleep stages did not appreciably contribute to morning plasma AD biomarker levels in these models, high EEG delta power is a prominent feature of non-rapid eye movement (NREM) stage N3 sleep. This is in marked contrast to the large effects that HR and particularly R_P had within these models, with lower overnight R_P contributing to greater morning plasma AD biomarker levels. Other than EEG delta power, the finding that neither EEG power bands nor sleep stages made a meaningful contribution to the optimal single predictors in sleep may be because R_P mediates the downstream effect of these variables. Conceptually, the synchronized low-frequency neural activity reflected in delta band power may serve as a key driving force for the process of glymphatic clearance[19,20], while sleep-related changes in extracellular volume fraction reflected in the R_P parameter[13,21] may regulate the effects of this driving force on fluid and solute transport within the brain parenchyma. If true, then R_P may represent a promising therapeutic target to increase glymphatic clearance of Aβ and tau.

It is important to point out the distinction between the changes in plasma AD biomarker levels observed through a single overnight period in the present study and changes in plasma AD biomarker levels that reflect steady-state alterations in AD-related pathology. For example, over the timescale of years, declining plasma Aβ42 levels and increasing p-tau levels occur with increasing Aβ plaque and tau pathological burden in AD. Within the setting of the present study,

overnight changes in plasma AD biomarker levels reflect the dynamics of both the release of Aβ and tau species into the brain interstitium, and their subsequent clearance to the CSF and the plasma in the overnight period. These dynamics are superimposed upon the existing steady-state Aβ42 and p-tau levels of each participant. Notably, despite seven participants being classified as 'amyloid positive', the 'amyloid-positive' covariate was non-significant in two of the three glymphatic models and only marginally significant in the third, suggesting that at short-timescales, changes in CSF-ISF exchange are unaffected by baseline Aβ42 and p-tau levels beyond what would be expected of concentration-dependent first-order kinetics. The converse – whether impaired overnight Aβ and tau clearance leads to increased AD pathological burden and long-term shifts in steady-state plasma AD biomarker levels – is a plausible hypothesis that will require a future prospective study.

The present findings have implications on the use and interpretations of plasma biomarkers in the diagnosis and assessment of AD in clinical populations. The use of diagnostic cutoff values to define disease features such as 'the presence of brain amyloid' assumes high intra-individual stability of these measures. Yet recent studies suggest that an individual's plasma AD biomarker levels may vary substantially over the course of several weeks[59], while different physiological parameters such as glomerular filtration rate, diabetes, or hypertension, may alter these levels[60]. Despite the sensitivity of plasma AD biomarker levels to exogenous and endogenous factors, ratios including such as Aβ42/Aβ40 and p-tau217/np-tau217 minimize these effects[24,60,61]. Our present findings suggest that within individuals over short timescales (weeks), sleep-related physiology does influence morning AD biomarker levels. While the scale of these effects appears modest in comparison to the changes in biomarker levels that are reported to be diagnostic of steady-state AD pathological burden, this suggests that physiological variables, such as sleep features, should be taken into consideration when

interpreting plasma AD biomarker results, particularly among participants with borderline plasma AD biomarker values.

Our findings showed that elements of sleep-active physiology, in particular brain parenchymal resistance, increase the clearance of AD biomarkers to plasma in overnight sleep in humans. Our **null model** and **glymphatic model** were estimated to predict morning AD biomarker levels from evening AD biomarker levels which is statistically superior to estimating those models on morning-to-evening differences or ratios of AD biomarker levels[62]. We further showed that in the wake state, sleep-like physiology is also capable of increasing Aβ ant tau clearance to the plasma. An important limitation of this study is that these predictions cannot be interpreted as causal without replication in a randomized control trial where the elements of sleep-active physiology can be manipulated against control conditions. Furthermore, our findings apply to healthy adults between 50 and 65 years old. Thus, while the prospect of AD primary and secondary prevention by targeting glymphatic clearance of Aβ and tau is promising, it remains to be shown that these findings translate to an older, higher risk population.

SUPPLEMENTAL METHODS AND RESULTS

Compartmental Pharmacokinetic Model Predictions

To define the effect that an overnight increase in glymphatic exchange would have on morning plasma AD biomarker levels, a 4-compartment model (**Figure 1A**) of solute transport and elimination from the ISF was constructed. A simplification of prior models[22], this model included the minimal compartments, transport and elimination pathways required to define the effect that a change in overnight glymphatic ISF-CSF exchange would have on morning plasma levels of Aβ and tau. This model was solved under both the **null model** and the **glymphatic model**. The **null model** assumed no sleep-active glymphatic exchange, rendering the rate constants k_{12} and k_{21} between ISF and CSF invariant across sleep and waking/sleep deprivation conditions. The **glymphatic model** assumed that these rate constants increase with sleep.

The movement of solute across the compartments in **Figure 1A** can be modeled using first-order kinetics with the published rate constants shown in **Table 1**. This leads to the following linear system of first-order differential equations where $f(t)$ is the time-dependent release of Aβ or tau into the ISF compartment,

$$\frac{dy_1}{dt} = -(k_{12} + k_{13} + k_{14})y_1 + k_{21}y_2 + f(t)$$

$$\frac{dy_2}{dt} = -(k_{21} + k_{23})y_2 + k_{12}y_1$$

$$\frac{dy_3}{dt} = -k_{3e}y_3 + k_{13}y_1 + k_{23}y_2$$

$$\frac{dy_4}{dt} = -k_{4e}y_4 + k_{14}y_1$$

and in matrix notation,

$$\frac{d\vec{y}}{dt} = A\vec{y} + f(t)\vec{u}_1$$

$$A = \begin{matrix} -(k_{12} + k_{13} + k_{14} + k_{15}) & k_{21} & 0 & 0 \\ k_{12} & -(k_{21} + k_{23}) & 0 & 0 \\ k_{13} & k_{23} & -k_{3e} & 0 \\ k_{14} & 0 & 0 & -k_{4e} \end{matrix}$$

where $\vec{u}_1$is the unit vector $(1,0,0,0,0)$.

The homogeneous solution must solve the following differential equation:

$$\frac{d\vec{y}}{dt} = A\vec{y} \qquad \textbf{Eq (1)}$$

Equation 1 was solved numerically using the Python function *scipy.integrate.odeint*. Peptides and proteins entering the ISF from any source will be cleared from the ISF to the various compartments in a time-dependent manner modeled by $\vec{y}(t)$. The **null model** assumes, in the absence of glymphatic exchange between the ISF and CSF, that the rate constants k_{21} and k_{12} are not time dependent. The **glymphatic model** assumes that these constants are time-varying and increase during sleep, reflecting the increased CSF solute influx and interstitial solute efflux observed in the rodent and human brain[13,15].

We then solved the simulation model for $\vec{y}(t)$ under the **null model** condition and then under the **glymphatic model**, reflected by an increase in the rate constants k_{21} and k_{12}, to define whether morning plasma Aβ and tau levels increase with more rapid overnight glymphatic CSF-ISF exchange. **Figure 1B** (top) shows compartmental concentrations of Aβ and tau over 24 hours following the release of each into the ISF at time $t = 0$ under the **null model** (solid lines), and under the **glymphatic model** (dashed lines). **Figure 1B** (bottom) shows Aβ and tau concentrations only within the plasma compartment. Within this model, both Aβ and tau

concentrations in the plasma increase in the **glymphatic model** compared to the **null model** over the entire 24 hr period.

Of final interest is the linear approximation of the morning:evening plasma level ratio in the plasma compartment

$$\frac{y(t_{AM})}{y(t_{PM})} \qquad \textbf{Eq (2)}$$

under the **null model** and **glymphatic model** assumptions. First we note that **Equation 1** can be solved by the fundamental matrix $\Phi(t)$. The columns of $\Phi(t)$ are $\vec{v}_i e^{\lambda_i t}$ where $\vec{v}_i$and λ_i are the eigenvectors and eigenvalues of A. Letting $\vec{y}_0$ denote the initial condition at $t = 0$, the solution for all $t \geq 0$ is given by:

$$\vec{y}(t) = \Phi(t)\Phi^{-1}(0)\vec{y}_0$$

Let $\Delta t = t_{AM} - t_{PM}$ represent the fixed time between the two blood samples. The ratio in **Equation 2** is proportional to $e^{\lambda_3 \Delta t}$ where λ_3 is the plasma compartment eigenvalue of the matrix A. In the **null model**, λ_3 is constant and therefore the morning plasma levels are directly proportional to the evening plasma levels. In the **glymphatic model**, λ_3 varies from wake to sleep through k_{21} and k_{12}. From the structure of matrix A, its eigenvalues are polynomials in the rate constants of **Table 1** that are linear in k_{12}, k_{21} and $k_{12}k_{21}$. Because these rate constants are all substantially < 1, a first-order approximation for λ_3 that retains only terms linear in the rate constants k_{12}, k_{21} can be used. The exponential term $e^{\lambda_3 \Delta t}$ can be approximated by a model linear in $\lambda_3 \Delta t$ around a narrow range of variation in λ_3. Equivalently, to a first-order approximation, $e^{\lambda_3 \Delta t}$ is well approximated by a model linear in $k_{21}\Delta t$ and $k_{12}\Delta t$. This yields the linear approximation:

$$y(t_{AM}) \propto y(t_{PM}) K \Delta t \qquad \textbf{Eq (3)}$$

where K is linear in k_{21} and k_{12}, and highlights the interaction term between evening levels of plasma biomarkers and glymphatic CSF-ISF exchange in the **glymphatic model** versus the

null model. In summary, in the **null model,** morning plasma levels are linearly dependent on evening plasma levels only, whereas the **glymphatic model** has a contribution from the interaction term between the evening plasma levels and the variable rate constants k_{21} and k_{12}.

Plasma AD biomarker assessment

The *APOE* genotyping, Aβ and tau plasma biomarkers were analyzed using mass spectrometry by C_2N Diagnostics[23]. The sample collection procedure was provided by C_2N Diagnostics. Venipuncture and blood draw from the antecubital fossa were performed using a 22-gauge butterfly needle to minimize red blood cell hemolysis. A total of 10 ml of blood was drawn into a K_2 EDTA Vacutainer. The blood was centrifuged for 15 min using a swinging bucket rotor at 500-700 x g with the brake on. Immediately after centrifugation, four 1.0 mL plasma samples were aliquoted into four Sarstedt 2.0 ml Micro Tubes without disrupting the plasma/cell interface when transferring plasma. A calibrated air-displacement hand-held pipette with a polypropylene pipette tip was used. After aliquoting plasma into the Sarstedt Micro Tubes, the tubes were immediately capped and frozen at -40°C. When the tubes were ready to be shipped to C_2N Diagnostics, they were packed into a plastic zip-lock bag with plenty of dry ice, placed in an absorbent towel and cryobox, and express couriered to C_2N Diagnostics priority overnight.

Multivariate mixed models

The R lme4 package was used for the linear mixed models. The multivariate linear mixed model was modeled in lme4[63].

Construction of Single Predictors

The objective of the single predictor approach using single-index regression[35] was to find the single linear combination of the regressor predictors in the group that best explained the data and its interaction with plasma biomarker levels using the **glymphatic model** by minimizing the

AIC of the model. The construction proceeded through two steps: **1)** selecting a subset of the predictor regressors from the appropriate group of regressors; **2)** running an optimization algorithm to find the weights for the linear combination that minimized the AIC of the **glymphatic model** on the data. A "best subset" selection procedure was used that evaluated all (2^k -1 for k predictor regressors in the group) models resulting from all possible combinations of the predictors[64]. For single predictors for the EEG spectral power features under the sleep condition (***Power**$_S$*) and the sleep deprivation/wake condition/wake condition (***Power**$_W$*) a total of 2^4-1, or 15 subsets of predictors from EEG delta and beta power bands, R_p, and HR were combined into a single predictor in the **glymphatic model** and weights optimized to maximize the log-likelihood of the sleep and sleep deprivation data, respectively. For single predictors in the hypnographic sleep stages under the sleep condition (***Hypno**$_S$*) a total of 2^6-1, or 63 subsets of predictors from EEG hypnogram stages N2, N3, REM, TST, R_p, and HR were combined into a single predictor in the **glymphatic model** and weights optimized to maximize the log-likelihood of the sleep data. Optimization was performed using the R optim function with Nelder-Mead optimization. Each optimization was run with multiple initial parameter values and the best result selected. Once the best single predictor subset of regressors and weights were determined for ***Power**$_S$*, ***Power**$_W$* and ***Hypno**$_S$*, Wald's p values and 95% CI were estimated on each of the weights using 1,000 bootstrap re-samples. The R package *lmeresampler* for bootstrap routines for nested linear mixed effects models was used to resample the data.

Multivariate model representing the null model and glymphatic models

The **null model** represented the null hypothesis that efflux of Aβ and tau from the ISF to plasma is not dependent on glymphatic exchange; that is, k_{12} and k_{21} are time-invariant. In this model, morning plasma levels of Aβ and tau species are assumed not to be influenced by either of the two groups (***Power***, ***Hypno***) of sleep-related predictors. Letting ***Conc**$_{AM}$* and ***Conc**$_{PM}$* denote the

morning and evening plasma levels of the five Aβ and tau biomarkers $A\beta_{40}$, $A\beta_{42}$, np-tau181, np-tau217 and p-tau181, respectively, the **null model** is the multivariate linear mixed model that regresses $\boldsymbol{Conc_{AM}}$ on $\boldsymbol{Comc_{PM}}$ with covariates of amyloid status, age, APOE-ε4 status, sex and study site, with participant ID as random intercept. This multivariate model was solved using R library lme4 after transforming the $\boldsymbol{Conc_{AM}}$ and $\boldsymbol{Conc_{PM}}$ into one-dimensional vectors and adding a variable *biomarker* to index these observations in the original data[63]. The *biomarker* variable was included in the model as an interaction term with the transformed $\boldsymbol{Conc_{PM}}$ and as a random slope.

The **glymphatic model** represented the alternative hypothesis that clearance of Aβ and tau species from the ISF to plasma is dependent on sleep-active glymphatic exchange, with k_{12} and k_{21} increasing overnight in the sleep condition. Three glymphatic models were tested, two for the sleep condition ($\boldsymbol{Power_S}$, $\boldsymbol{Hypno_S}$) and one for the sleep deprivation/wake condition ($\boldsymbol{Power_W}$). The predictors $\boldsymbol{Power_S}$ and $\boldsymbol{Power_W}$ denote single predictors constructed from the linear combination of R_p, EEG power bands and HR during the sleep and sleep deprivation (wake) conditions, respectively. The predictor $\boldsymbol{Hypno_S}$ denotes the single predictor constructed from the linear combination of R_p, EEG hypnogram stages and HR during the sleep condition. The two sleep **glymphatic models** added to the **null model** the predictors $\boldsymbol{Power_S}$ and $\boldsymbol{Hypno_S}$ and their respective interaction terms with evening levels of plasma amyloid and tau $\boldsymbol{Power_S * Conc_{PM}}$ and $\boldsymbol{Hypno_S * Conc_{PM}}$. The sleep deprivation/wake **glymphatic model** added to the **null model** the predictor $\boldsymbol{Power_W}$ and the interaction term $\boldsymbol{Power_W * Conc_{PM}}$. The R Anova function in the car package was used for analysis of deviance using a type III Wald Chi-squre test for the interaction effects.

The likelihood ratio test (LRT) was used for significance testing of the **glymphatic model** versus the **null model**. Of particular interest was the percent of the residual variation in **null model** that was explained by the **glymphatic model**; that is, the additional variation explained by including one of the single predictors ***Power*$_S$**, ***Power*$_W$** or ***Hypno*$_S$** in the **glymphatic model** under the normal sleep or sleep deprivation/wake conditions. The residual variation of each model was computed from the sum of the square difference between the observed morning plasma AD biomarker levels and the fitted morning plasma levels for Aβ_{40}, Aβ_{42}, np-tau181, np-tau217 and p-tau181 individually using maximum likelihood. Letting RSS_0 and RSS denote these two quantities for the **null model** and a **glymphatic model**, $1 - \frac{RSS}{RSS_0}$ gives the R^2 of the multivariate linear mixed models[65]. Confidence intervals for these R^2 estimates were computed using 1,000 bootstrap resamples.

FIGURES

Figure 1. Four-compartment model of brain to plasma fluid exchange

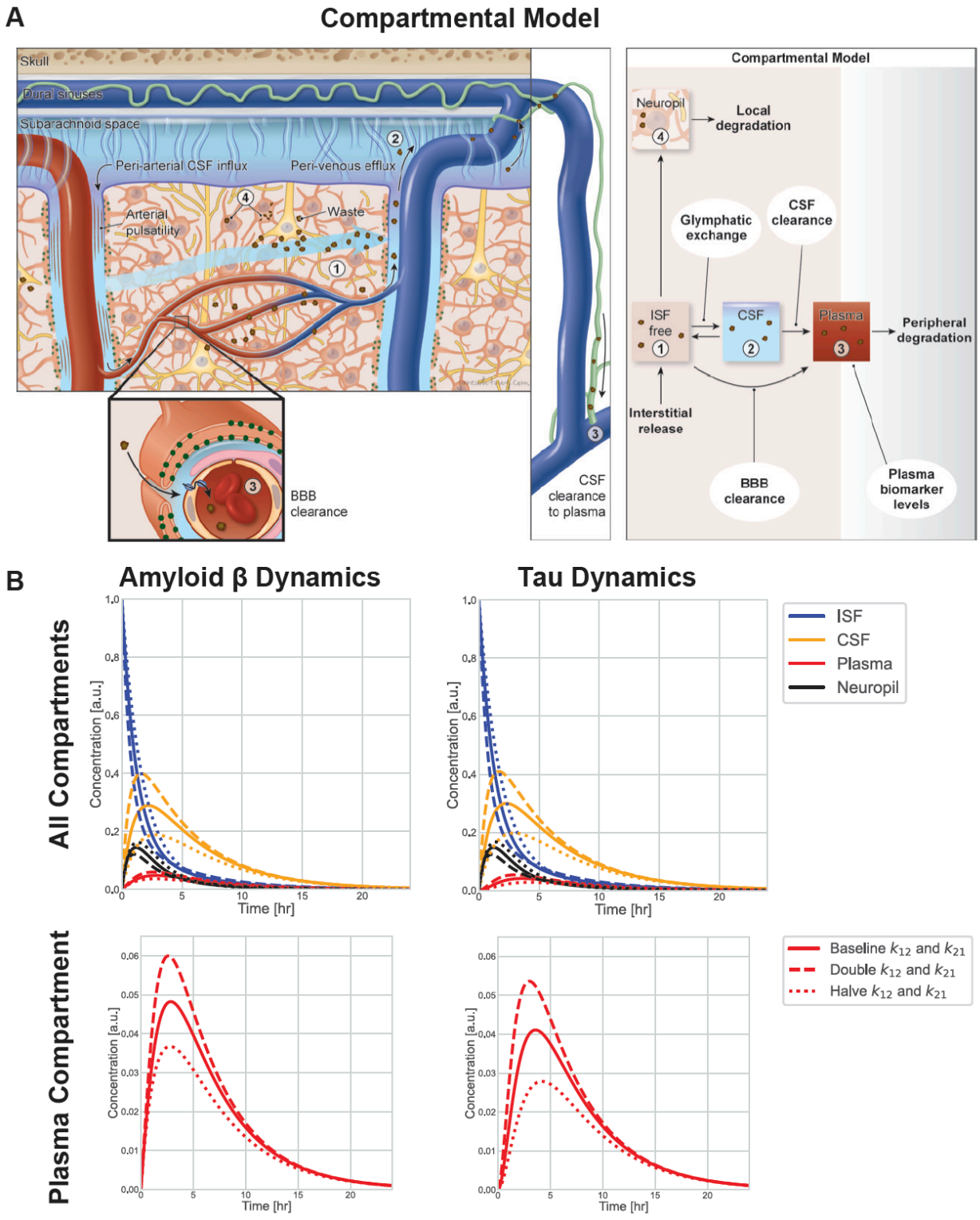

Figure 2. Study schematic and CONSORT diagram.

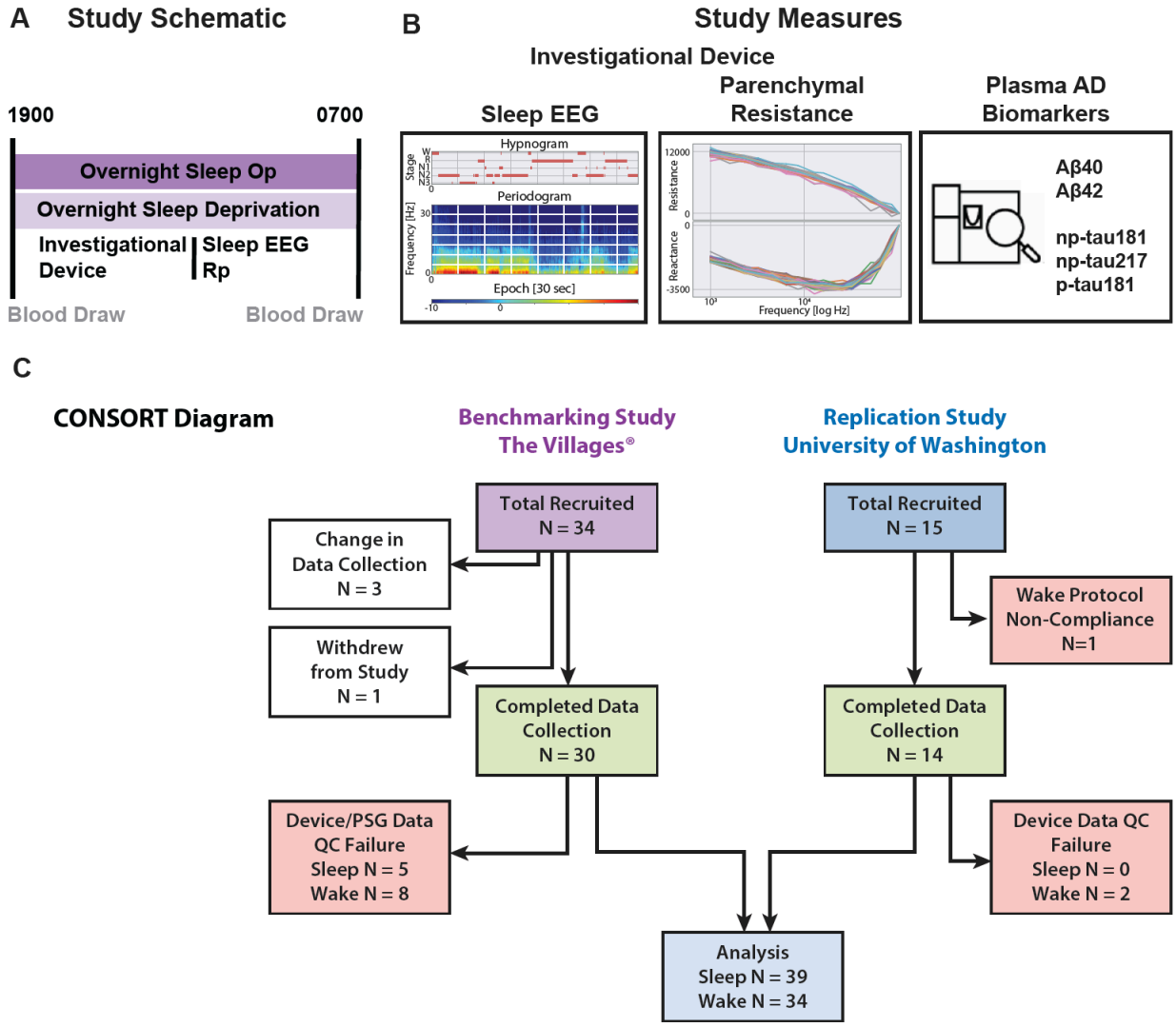

Figure 3.

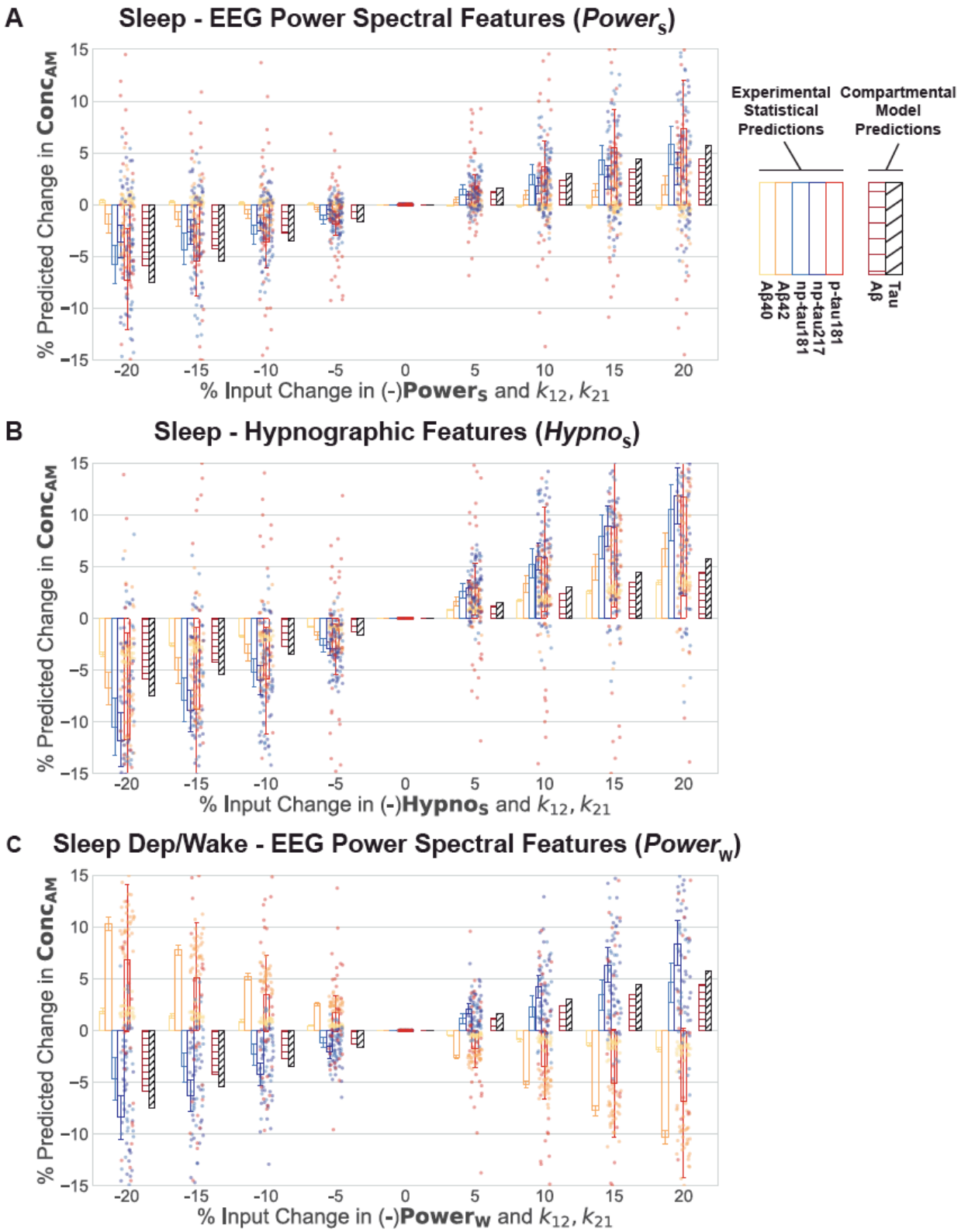

TABLES

Table 1: Compartment rate constants of amyloid β and tau transport*

Rate Constant	Process	Amyloid Value	Tau Value
k_{12}	Glymphatic interstitial solute efflux	$0.151\ hr^{-1}$	$0.151\ hr^{-1}$
k_{21}	Glymphatic CSF solute influx	$0.151\ hr^{-1}$	$0.151\ hr^{-1}$
k_{13}	Blood-brain barrier solute efflux	$0.38 \times 0.1\ hr^{-1}$	0
k_{14}	Local cellular uptake and degradation within the neuropil	$0.38 \times 0.9\ hr^{-1}$	$0.38 \times 0.9\ hr^{-1}$
k_{23}	CSF clearance	$0.151\ hr^{-1}$	$0.151\ hr^{-1}$
k_{3e}	Peripheral elimination	$1.0\ hr^{-1}$	$1.0\ hr^{-1}$
k_{4e}	Local cellular elimination	$1.0\ hr^{-1}$	$1.0\ hr^{-1}$

*Published rate constants[22].

Table 2. Clinical study demographic information*

Study	Age	Sex (F/M)	APOE-e4 (+/-)	Amyloid Plaque Status (+/-)	MoCA	GDS
Villages	61.9 (2.7)	13/12	7/18	7/18	27.9 (1.2)	0.7 (1.2)
University of Washington	55.6 (4.6)	7/7	5/9	0/14	28.6 (1.2)	0.6 (1.2)
Combined	59.6 (4.6)	20/19	12/27	7/32	28.1 (1.2)	0.7 (1.2)

*Values are Mean (SD) or count. MoCA, Montreal Cognitive Assessment; GDS, Geriatric Depression Scale. Amyloid plaque status determined using C_2N PrecivityAD test with cutoff of 0.089[24,26,36].

Table 3. Morning and evening plasma levels of Aβ ($A\beta_{40}$, $A\beta_{42}$) and tau species (np-tau181, np-tau217, p-tau181).*

Condition	Plasma Biomarker [units]	Morning Plasma Levels ($Conc_{AM}$)	Evening Plasma Levels ($Conc_{PM}$)	Differences (evening – morning)
Sleep	$A\beta_{40}$ [pg/mL]	406.64 (56.12)	422.66 (56.44)	16.03 (28.52)
	$A\beta_{42}$ [pg/mL]	39.48 (7.79)	41.95 (8.47)	2.48 (4.79)
	np-tau181 [pg/mL]	71.94 (23.25)	74.36 (30.94)	2.41 (14.40)
	np-tau217 [pg/mL]	87.23 (27.38)	90.54 (36.90)	3.30 (20.71)
	p-tau181 [pg/mL]	10.59 (4.44)	11.42 (5.59)	0.83 (2.20)
Sleep Deprivation / Wake	$A\beta_{40}$ [pg/mL]	389.41 (48.77)	394.96 (52.58)	5.55 (32.46)
	$A\beta_{42}$ [pg/mL]	38.22 (5.83)	39.86 (6.23)	1.64 (2.97)
	np-tau181 [pg/mL]	64.66 (23.45)	74.96 (34.06)	10.30 (16.21)
	np-tau217 [pg/mL]	77.83 (26.29)	92.14 (39.35)	14.31 (19.58)
	p-tau181 [pg/mL]	9.81 (4.90)	11.22 (5.47)	1.41 (2.60)

*Data shown as mean (SD).

Table 4. Optimal predictors and weights for predicting morning plasma levels of $A\beta_{40}$, $A\beta_{42}$, np-tau181, np-tau217, p-tau181 in sleep and sleep deprivation conditions.*

Condition and Predictor	Selected Predictors	Estimate	CI	Wald's P
Sleep Condition *Power$_S$*	R_p	0.987	0.749 – 1.225	**<0.001**
	EEG delta power	-0.161	-0.226 – -0.096	**<0.001**
Sleep Condition *Hypno$_S$*	R_p	0.730	0.673 – 0.788	**<0.001**
	N2	-0.001	-0.082 – 0.081	0.982
	REM	0.002	-0.089 – 0.093	0.968
	HR	0.683	0.625 – 0.741	**<0.001**
Sleep Deprivation/Wake *Power$_W$*	EEG delta power	0.431	0.315 – 0.547	**<0.001**
	EEG beta power	0.346	0.249 – 0.442	**<0.001**
	HR	0.834	0.724 – 0.943	**<0.001**

*CI, 95% Confidence Interval; R_p, Parenchymal Resistance; HR, Heart Rate; EEG, Electroencephalography; ***Power$_S$*** and ***Power$_W$***, single predictors constructed from the linear combination of R_p, EEG power bands and heart rate during the sleep and sleep deprivation (wake) conditions, respectively; ***Hypno$_S$***, single predictor constructed from the linear combination of R_p, EEG hypnogram features and heart rate during the sleep condition. Selected predictors and estimated weights were selected using optimization to minimize the AIC of the glymphatic model. For ***Hypno$_S$***, both N2 and REM are near zero and insignificant based on 95% CI and Wald's P value. **Bolded P values reflect significant associations at P < 0.05**.

Table 5: Prediction of morning plasma levels of $A\beta_{40}$, $A\beta_{42}$, np-tau181, np-tau217, p-tau181 following overnight sleep using the *null model* and the *glymphatic model* with $Power_S$.*

Model	Predictor Group	Predictor		Estimate	DF	CI	P
Null Model	Fixed Effects	Amyloid-positive		0.615	33	-0.275 – 1.505	0.169
		Age		0.174	33	0.069 – 0.279	**0.002**
		Gender (male)		0.438	33	-0.299 – 1.175	0.235
		APOE-ε4 (positive)		-0.188	33	-0.941 – 0.564	0.614
		Study (Villages)		-0.836	33	-1.905 – 0.233	0.121
		Evening Plasma Biomarker Effects	Aβ40: $Conc_{PM}$	0.953	143	0.931 – 0.975	**<0.001**
			Aβ42: $Conc_{PM}$	0.882	143	0.842 – 0.922	**<0.001**
			np-tau181: $Conc_{PM}$	0.882	143	0.833 – 0.931	**<0.001**
			np-tau217: $Conc_{PM}$	0.868	143	0.808 – 0.929	**<0.001**
			p-tau181: $Conc_{PM}$	0.729	143	0.653 – 0.805	**<0.001**
	Random Effects	σ^2		1.080			
		$\tau_{11\ pid\ Ab42}$		18.358			
		$\tau_{11\ pid\ np\text{-}tau181}$		166.057			
		$\tau_{11\ pid\ np\text{-}tau217}$		362.761			
		$\tau_{11\ pid\ p\text{-}tau181}$		1.177			
Glymphatic Model	Fixed Effects	Amyloid-positive		0.416	33	-0.420 – 1.252	0.319
		Age		0.179	33	0.082 – 0.276	**0.001**
		Gender (male)		0.295	33	-0.404 – 0.994	0.397
		APOE-ε4 (positive)		0.052	33	-0.645 – 0.750	0.879
		Study (Villages)		-1.272	33	-2.286 – -0.259	**0.015**
		Predictor Effects	Aβ40: $Power_S$	92.020	133	7.897 – 176.143	**0.032**
			Aβ42: $Power_S$	29.969	133	14.890 – 45.048	**<0.001**
			np-tau181: $Power_S$	53.762	133	37.305 – 70.219	**<0.001**
			np-tau217: $Power_S$	69.955	133	49.984 – 89.926	**<0.001**
			p-tau181: $Power_S$	24.362	133	11.160 – 37.563	**<0.001**
		Evening Plasma Biomarker Effects	Aβ40: $Conc_{PM}$	0.985	133	0.802 – 1.168	**<0.001**
			Aβ42: $Conc_{PM}$	1.402	133	1.068 – 1.735	**<0.001**
			np-tau181: $Conc_{PM}$	1.404	133	1.020 – 1.788	**<0.001**
			np-tau217: $Conc_{PM}$	1.472	133	1.048 – 1.895	**<0.001**
			p-tau181: $Conc_{PM}$	2.781	133	1.757 – 3.806	**<0.001**
		Evening Biomarker: Predictor Interactions	Aβ40: $Power_S$: $Conc_{PM}$	-0.197	133	-0.499 – 0.104	0.197
			Aβ42: $Power_S$: $Conc_{PM}$	-0.853	133	-1.310 – -0.396	**<0.001**
			np-tau181: $Power_S$: $Conc_{PM}$	-1.029	133	-1.550 – -0.507	**<0.001**
			np-tau217 $Power_S$: $Conc_{PM}$	-1.223	133	-1.796 – -0.649	**<0.001**
			p-tau181: $Power_S$: $Conc_{PM}$	-2.864	133	-4.262 – -1.466	**<0.001**
	Random Effects	σ^2		0.850			
		$\tau_{11\ pid\ Ab42}$		17.572			
		$\tau_{11\ pid\ np\text{-}tau181}$		99.653			
		$\tau_{11\ pid\ np\text{-}tau217}$		214.132			
		$\tau_{11\ pid\ p\text{-}tau181}$		0.919			

*DF, degrees of freedom; CI, 95% confidence interval; P, p-value; $Power_S$, single predictor constructed from the linear combination of R_p, EEG power bands and heart rate during the sleep; $Conc_{PM}$, evening plasma level; Amyloid positive, positive amyloid plasma test; UF, University of Florida study site; EEG, Electroencephalography; R_P, Parenchymal Resistance; HR, Heart Rate; σ^2, residual variance; τ_{11}, random slope variance; **Bolded P values reflect significant associations at P < 0.05**. Shaded cells demark random effects and potential biological confounders.

Table 6. Estimate for single predictor coefficient in the glymphatic model in sleep and sleep deprivation evaluated at the mean evening plasma AD biomarker levels.*

Glymphatic Model	Factor	Estimate at Mean Value of $Conc_{PM}$ for Biomarker	P of Main Effect	P of Interaction Effect
Sleep Condition P_s	$(1+\overline{Conc}_{PM,Ab40})$ **$Power_S$**	8.580	**0.032**	0.197
	$(1+\overline{Conc}_{PM,Ab42})$ **$Power_S$**	-5.807	**<0.001**	**<0.001**
	$(1+\overline{Conc}_{PM,nTau181})$ **$Power_S$**	-39.173	**<0.001**	**<0.001**
	$(1+\overline{Conc}_{PM,nTau217})$ **$Power_S$**	-22.307	**<0.001**	**<0.001**
	$(1+\overline{Conc}_{PM,pTau181})$ **$Power_S$**	-8.353	**<0.001**	**<0.001**
Sleep Condition H_s	$(1+\overline{Conc}_{PM,Ab40})$ **$Hypno_S$**	-54.772	**0.014**	0.057
	$(1+\overline{Conc}_{PM,Ab42})$ **$Hypno_S$**	-11.111	**<0.001**	**<0.001**
	$(1+\overline{Conc}_{PM,nTau181})$ **$Hypno_S$**	-41.098	**<0.001**	**0.002**
	$(1+\overline{Conc}_{PM,nTau217})$ **$Hypno_S$**	-38.309	**<0.001**	**<0.001**
	$(1+\overline{Conc}_{PM,pTau181})$ **$Hypno_S$**	-8.661	**<0.001**	**<0.001**
Sleep Deprivation/Wake P_w	$(1+\overline{Conc}_{PM,Ab40})$ **$Power_W$**	21.551	**0.007**	0.323
	$(1+\overline{Conc}_{PM,Ab42})$ **$Power_W$**	12.053	**0.024**	0.544
	$(1+\overline{Conc}_{PM,nTau181})$ **$Power_W$**	-14.628	**0.001**	**0.003**
	$(1+\overline{Conc}_{PM,nTau217})$ **$Power_W$**	-20.292	**0.004**	**<0.001**
	$(1+\overline{Conc}_{PM,pTau181})$ **$Power_W$**	-0.072	0.094	**0.013**

Table 7: Likelihood ratio test of the glymphatic model versus the null model.*

Condition and Added Predictor	Model	DF	AIC	BIC	logLik	LRT	P
Sleep Condition, *Power*$_S$	Glymphatic	37	1234.1	1353.6	-580.0		
	Null	27	1270.8	1358.0	-608.4	56.70	**<0.001**
Sleep Condition, *Hypno*$_S$	Glymphatic	37	1229.86	1349.42	-577.93		
	Null	27	1273.51	1360.75	-609.76	63.65	**<0.001**
Sleep Deprivation/Wake *Power*$_W$	Glymphatic	37	1106.96	1222.10	-516.48		
	Null	27	1141.14	1225.16	-543.57	54.18	**<0.001**

*DF, degrees of freedom; AIC, Akaike Information Criteria; BIC, Bayesian Information Criteria; logLik, log likelihood; LRT, log likelihood ratio; P, p-value; ***Power*$_S$** and ***Power*$_W$**, single predictors constructed from the linear combination of R_p, EEG power bands and heart rate during the sleep and sleep deprivation (wake) conditions, respectively; ***Hypno*$_S$**, single predictor constructed from the linear combination of R_p, EEG hypnogram and heart rate during the sleep condition; **Bolded P values reflect significant LRT at P < 0.05**.

Table 8. Percent of variance in morning plasma AD biomarker levels explained by the glymphatic model versus the null model.*

Condition and Added Predictor	Plasma Biomarker	Percent of Variation Explained by Null Model	Percent of Null Residual Variation Explained by Glymphatic Model	CI	P
Sleep Condition *Power$_S$*	Ab40	91.2%	48.4%	24.2% – 72.6%	**<0.001**
	Ab42	94.9%	43.3%	17.9% – 68.7%	**0.001**
	np-tau217	98.1%	23.7%	-11.7% – 59.2%	0.189
	np-tau181	97.6%	30.5%	-0.4% – 61.5%	0.053
	p-tau181	77.4%	31.8%	13.8% – 49.9%	**0.001**
Sleep Condition *Hypno$_S$*	Ab40	72.7%	66.8%	37.1% – 96.5%	**<0.001**
	Ab42	85.1%	61.5%	27.2% – 95.8%	**<0.001**
	np-tau217	94.7%	37.1%	-19.9% – 94.2%	0.202
	np-tau181	92.7%	48.2%	1.1% – 95.2%	**0.045**
	p-tau181	62.0%	46.1%	4.4% – 87.9%	**0.03**
Sleep Deprivation/Wake *Power$_W$*	Ab40	62.0%	4.8%	-38.1% – 47.8%	0.825
	Ab42	49.0%	-20.8%	-75.9% – 34.4%	0.461
	np-tau217	76.8%	-22.5%	-82.0% – 37.0%	0.459
	np-tau181	74.2%	-26.7%	-85.4% – 32.0%	0.374
	p-tau181	31.7%	1.8%	-29.3% – 33.0%	0.907

*CI, 95% confidence interval; P, p-value; ***Power$_S$*** and ***Power$_W$***, single predictors constructed from the linear combination of R_p, EEG power bands and heart rate during the sleep and sleep deprivation (wake) conditions, respectively; ***Hypno$_S$***, single predictor constructed from the linear combination of R_p, EEG hypnogram and heart rate during the sleep condition. **Bolded P values reflect significant values at P < 0.05**.

Table 9. Prediction of morning plasma levels of $A\beta_{40}$, $A\beta_{42}$, np-tau181, np-tau217, p-tau181 following sleep using the *null model* and the *glymphatic model* with *Hypno$_S$*.*

Model	Predictor Group	Predictor		Estimate	DF	CI	P
Null Model	Fixed Effects	Amyloid-positive		0.615	33	-0.275 – 1.505	0.169
		Age		0.174	33	0.069 – 0.279	**0.002**
		Gender (male)		0.438	33	-0.299 – 1.175	0.235
		APOE-ε4 (positive)		-0.188	33	-0.941 – 0.564	0.614
		Study (Villages)		-0.836	33	-1.905 – 0.233	0.121
		Evening Plasma Biomarker Effects	Aβ40: ***Conc$_{PM}$***	0.953	143	0.931 – 0.975	**<0.001**
			Aβ42: ***Conc$_{PM}$***	0.882	143	0.842 – 0.922	**<0.001**
			np-tau181: ***Conc$_{PM}$***	0.882	143	0.833 – 0.931	**<0.001**
			np-tau217: ***Conc$_{PM}$***	0.868	143	0.808 – 0.929	**<0.001**
			p-tau181: ***Conc$_{PM}$***	0.729	143	0.653 – 0.805	**<0.001**
	Random Effects	σ^2		1.080			
		$T_{11\ pid\ Ab42}$		18.358			
		$T_{11\ pid\ np\text{-}tau181}$		166.057			
		$T_{11\ pid\ np\text{-}tau217}$		362.761			
		$T_{11\ pid\ p\text{-}tau181}$		1.177			
Glymphatic Model	Fixed Effects	Amyloid-positive		0.801	33	0.031 – 1.571	**0.042**
		Age		0.171	33	0.082 – 0.260	**<0.001**
		Gender (male)		0.363	33	-0.286 – 1.012	0.264
		APOE-e4 (positive)		-0.032	33	-0.668 – 0.604	0.920
		Study (Villages)		-1.098	33	-2.068 – -0.128	**0.028**
		Predictor Effects	Ab40: ***Hypno$_S$***	62.836	133	12.762 – 112.911	**0.014**
			Ab42: ***Hypno$_S$***	30.695	133	18.539 – 42.852	**<0.001**
			np-tau181: ***Hypno$_S$***	46.736	133	34.108 – 59.364	**<0.001**
			np-tau217: ***Hypno$_S$***	56.344	133	42.101 – 70.587	**<0.001**
			p-tau181: ***Hypno$_S$***	28.883	133	17.422 – 40.344	**<0.001**
		Evening Plasma Biomarker Effects	Ab40: ***Conc$_{PM}$***	1.214	133	0.872 – 1.555	**<0.001**
			Ab42: ***Conc$_{PM}$***	2.084	133	1.479 – 2.689	**<0.001**
			np-tau181: ***Conc$_{PM}$***	2.090	133	1.360 – 2.819	**<0.001**
			np-tau217: ***Conc$_{PM}$***	1.927	133	1.080 – 2.775	**<0.001**
			p-tau181: ***Conc$_{PM}$***	4.809	133	3.241 – 6.377	**<0.001**
		Evening Biomarker: Predictor Interactions	Ab40: ***Hypno$_S$***: ***Conc$_{PM}$***	-0.278	133	-0.565 – 0.009	0.057
			Ab42: ***Hypno$_S$***: ***Conc$_{PM}$***	-0.996	133	-1.454 – -0.539	**<0.001**
			np-tau181: ***Hypno$_S$***: ***Conc$_{PM}$***	-1.144	133	-1.716 – -0.572	**<0.001**
			np-tau217 ***Hypno$_S$***: ***Conc$_{PM}$***	-1.076	133	-1.737 – -0.415	**0.002**
			p-tau181: ***Hypno$_S$***: ***Conc$_{PM}$***	-3.287	133	-4.525 – -2.048	**<0.001**
	Random Effects	σ^2		0.782			
		$T_{11\ pid\ Ab42}$		17.257			
		$T_{11\ pid\ np\text{-}tau181}$		100.330			
		$T_{11\ pid\ np\text{-}tau217}$		238.475			
		$T_{11\ pid\ p\text{-}tau181}$		0.899			

*DF, degrees of freedom; CI, 95% confidence interval; P, p-value; ***Hypno$_S$***, single predictor constructed from the linear combination of R_p, EEG hypnogram and heart rate during the sleep; ***Conc$_{PM}$***, evening plasma level; Amyloid positive, positive amyloid plasma test; UF, University of Florida study site; EEG, Electroencephalography; R_P, Parenchymal Resistance; HR, Heart Rate; σ^2, residual variance; τ_{11}, random slope variance; **Bolded P values reflect significant associations at P < 0.05**. Shaded cells demark random effects and potential biological confounders.

Table 10. Prediction of morning plasma levels of $A\beta_{40}$, $A\beta_{42}$, np-tau181, np-tau217, p-tau181 following sleep using the *null model* and the *glymphatic model* with $Power_W$.*

Model	Predictor Group	Predictor		Estimate	DF	CI	P
Null Model	Fixed Effects	Amyloid positive		0.706	28	-0.792 – 2.203	0.343
		Age		0.109	28	-0.053 – 0.272	0.179
		Gender (male)		-0.098	28	-1.205 – 1.009	0.858
		APOE-e4 (positive)		-0.263	28	-1.417 – 0.890	0.644
		Study (Villages)		-0.717	28	-2.207 – 0.772	0.333
		Evening Plasma Biomarker Effects	Ab40: $Conc_{PM}$	0.974	127	0.947 – 1.002	**<0.001**
			Ab42: $Conc_{PM}$	0.928	127	0.880 – 0.976	**<0.001**
			np-tau181: $Conc_{PM}$	0.802	127	0.751 – 0.852	**<0.001**
			np-tau217: $Conc_{PM}$	0.788	127	0.738 – 0.837	**<0.001**
			p-tau181: $Conc_{PM}$	0.748	127	0.615 – 0.882	**<0.001**
	Random Effects	σ^2		2.894			
		$\tau_{11\ pid\ Ab42}$		5.036			
		$\tau_{11\ pid\ np\text{-}tau181}$		140.916			
		$\tau_{11\ pid\ np\text{-}tau217}$		202.924			
		$\tau_{11\ pid\ p\text{-}tau181}$		3.019			
Glymphatic Model	Fixed Effects	Amyloid positive		0.280	28	-1.271 – 1.832	0.714
		Age		0.145	28	-0.021 – 0.311	0.085
		Gender (male)		-0.234	28	-1.354 – 0.887	0.672
		APOE-e4 (positive)		-0.424	28	-1.666 – 0.818	0.490
		Study (Villages)		-0.929	28	-3.530 – -0.327	**0.020**
		Predictor Effects	Ab40: $Power_W$	68.756	117	19.44 – 118.07	**0.007**
			Ab42: $Power_W$	16.484	117	2.168 – 30.799	**0.024**
			np-tau181: $Power_W$	21.738	117	7.287 – 36.189	**0.004**
			np-tau217: $Power_W$	26.330	117	11.540 – 41.120	**0.001**
			p-tau181: $Power_W$	11.680	117	-2.019 – 25.380	0.094
		Evening Plasma Biomarker Effects	Ab40: $Conc_{PM}$	0.945	117	0.568 – 1.322	**<0.001**
			Ab42: $Conc_{PM}$	0.924	117	0.349 – 1.499	**0.002**
			np-tau181: $Conc_{PM}$	1.545	117	1.080 – 2.009	**<0.001**
			np-tau217: $Conc_{PM}$	1.301	117	0.816 – 1.787	**<0.001**
			p-tau181: $Conc_{PM}$	2.494	117	1.137 – 3.850	**<0.001**
		Evening Biomarker: Predictor Interactions	Ab40: $Power_W$: $Conc_{PM}$	-0.120	117	-0.358 – 0.119	0.323
			Ab42: $Power_W$: $Conc_{PM}$	-0.111	117	-0.473 – 0.251	0.544
			np-tau181: $Power_W$: $Conc_{PM}$	-0.561	117	-0.838 – -0.283	**<0.001**
			np-tau217 $Power_W$: $Conc_{PM}$	-0.445	117	-0.734 – -0.155	**0.003**
			p-tau181: $Power_W$: $Conc_{PM}$	-1.047	117	-1.865 – -0.229	**0.013**
	Random Effects	σ^2		2.751			
		$\tau_{11\ pid\ Ab42}$		3.379			
		$\tau_{11\ pid\ np\text{-}tau181}$		79.000			
		$\tau_{11\ pid\ np\text{-}tau217}$		126.237			
		$\tau_{11\ pid\ p\text{-}tau181}$		1.982			

*DF, degrees of freedom; CI, 95% confidence interval; P, p-value; ***$Power_W$***, single predictor constructed from the linear combination of R_p, EEG power bands and heart rate during the sleep deprivation; ***$Conc_{PM}$***, evening plasma level; Amyloid positive, positive amyloid plasma test; UF, University of Florida study site; EEG, Electroencephalography; R_P, Parenchymal Resistance; HR, Heart Rate; σ^2, residual variance; τ_{11}, random slope variance; **Bolded P values reflect significant associations at P < 0.05**. Shaded cells demark random effects and potential biological confounders.

Table 11. Analysis of deviance using type III Wald Chi-square test for glymphatic model interaction effects.*

Glymphatic Model	Factor	Chi-squared	DF	P
Sleep Condition *Power$_S$*	Amyloid positive	1.025	1	0.311
	Age	14.190	1	**<0.001**
	Gender (male)	0.736	1	0.391
	APOE-e4 (positive)	0.023	1	0.879
	Study (Villages)	6.520	1	**0.011**
	Biomarker: ***Power$_S$***	37.871	5	**<0.001**
	Biomarker: ***Conc$_{PM}$***	698.587	5	**<0.001**
	Biomarker: ***Power$_S$*:Conc$_{PM}$**	29.099	5	**<0.001**
Sleep Condition *Hypno$_S$*	Amyloid positive	4.477	1	**0.034**
	Age	15.366	1	**<0.001**
	Gender (male)	1.292	1	0.256
	APOE-e4 (positive)	0.010	1	0.920
	Study (Villages)	5.300	1	**0.021**
	Biomarker: ***Hypno$_S$***	42.044	5	**<0.001**
	Biomarker: ***Conc$_{PM}$***	676.594	5	**<0.001**
	Biomarker: ***Hypno$_S$*:Conc$_{PM}$**	36.903	5	**<0.001**
Sleep deprivation/Wake *Power$_W$*	Amyloid positive	0.137	1	0.711
	Age	3.198	1	**0.074**
	Gender (male)	0.183	1	0.669
	APOE-e4 (positive)	0.488	1	0.485
	Study (Villages)	6.086	1	**0.014**
	Biomarker: ***Power$_W$***	45.891	5	**<0.001**
	Biomarker: ***Conc$_{PM}$***	401.465	5	**<0.001**
	Biomarker: ***Power$_W$*: Conc$_{PM}$**	19.185	5	**0.002**

*DF, degrees of freedom; P, p-value; ***Power$_S$***, single predictor constructed from the linear combination of R_p, EEG power bands and heart rate during the sleep***; Hypno$_S$***, single predictor constructed from the linear combination of R_p, EEG hypnogram and heart rate during the sleep***; Power$_W$***, single predictor constructed from the linear combination of R_p, EEG power bands and heart rate during the sleep deprivation; ***Conc$_{PM}$***, evening plasma level; **Bolded P values reflect significant associations at P < 0.05**.

FIGURE LEGENDS

Figure 1. Compartmental pharmacokinetic model defining the clearance of interstitial Aβ and tau clearance to the plasma. (A) Amyloid β (Aβ) and tau that enter the ISF compartment (**1**) are cleared from the ISF via local cellular uptake (**1 → 4**) and degradation, blood-brain barrier efflux (**1 → 3**), or glymphatic efflux to the CSF (**1 → 2**). CSF solutes may recirculate back into the brain interstitium (**2 → 1**) or be cleared by CSF efflux pathways to the plasma (**2 → 3**) from whence peripheral degradation occurs. **(B)** Compartment concentrations of Aβ (left) and tau (right) over 24 hours following release of 1 arbitrary unit of Aβ peptide or tau protein into the ISF at time 0 hr. Solid lines show compartment concentrations under the **null model**, with time-invariant exchange between the CSF (**2**) and ISF (**1**) compartments. Long dashed lines show change in compartment concentrations when glymphatic efflux/influx rate constants k_{12} and k_{21} were increased by a factor of 2. Dotted lines show change in compartment concentrations when glymphatic efflux/influx rate constants k_{12} and k_{21} were slowed by a factor of 2. Note that accelerating ISF-CSF exchange, consistent with the glymphatic model, leads to higher plasma levels of Aβ and tau throughout the 24-hour period. Slowing ISF-CSF exchange led to lower plasma levels of Aβ and tau throughout the 24-hour period.

Figure 2. Study schematic and CONSORT diagram.

The Benchmarking Study conducted at The Villages® and the Replication study conducted at the University of Washington were **(A)** randomized cross-over assignment of overnight sleep opportunity and overnight sleep deprivation designed to define the relationship between parenchymal resistance (R_P) and glymphatic function. **(B)** Reported here are the overnight investigational device recordings of R_P, EEG and HR, and blood analysis of amyloid β and tau levels (Aβ40, Aβ42, np-tau181, np-tau217 and p-tau181). **(C)** The Benchmarking Study enrolled 34 participants of which 30 completed both visits. Three were censored due to changes in

device data collection and sensor locations. One withdrew following the first MRI scan. Of the 30 that completed the study, 5 overnight sleep visits and 8 overnight wake visits failed the data quality control (QC) criteria to provide sufficient artifact free data to yield results. This resulted in 25 sleep and 22 wake complete data sets. The Replication Study enrolled 14 participants. All 14 completed the study, of which 3 wake visits failed the data QC criteria and no sleep visit failed.

Figure 3. Comparison of glymphatic model and multicompartment model predictions of morning plasma level. The percent change prediction in morning plasma level $\boldsymbol{Conc_{AM}}$ of AD biomarkers $A\beta_{40}$, $A\beta_{42}$, np-tau181, np-tau217, p-tau181 resulting from a change in the single predictors $\boldsymbol{Power_S}$ **(a)**, $\boldsymbol{Hypno_S}$ **(b)**, and $\boldsymbol{Power_W}$ **(c)** of the glymphatic model are compared against the percent change in the amyloid β and tau multicompartment model from a corresponding change in the rate constants k_{12} and k_{21}. Predicted mean and 95% confidence intervals for $A\beta_{40}$, $A\beta_{42}$, np-tau181, np-tau217, p-tau181 at each % change in the single predictor are shown in order as the first five bars alongside the glymphatic model predictions for that % change. Multicompartment model predictions for amyloid β and tau at each % change of the rate constants k_{12} and k_{21} are shown in order as the last two hatched bars. The change in the negative of the single predictors are shown for comparison with the change in the rate constants. For example, a 20% increase in the negative predictor corresponds to a 20% decrease in the actual predictor. AD biomarkers in the glymphatic model with coefficients having a P values < 0.05 were $A\beta_{42}$, np-tau181, np-tau217, p-tau181 for $\boldsymbol{Power_S}$ and $\boldsymbol{Hypno_S}$, and np-tau181, np-tau217 for $\boldsymbol{Power_W}$.

REFERENCES

1 Robbins, R. *et al.* Examining sleep deficiency and disturbance and their risk for incident dementia and all-cause mortality in older adults across 5 years in the United States. *Aging (Albany NY)* **13**, 3254-3268 (2021). https://doi.org/10.18632/aging.202591

2 Lutsey, P. L. *et al.* Sleep characteristics and risk of dementia and Alzheimer's disease: The Atherosclerosis Risk in Communities Study. *Alzheimers Dement* **14**, 157-166 (2018). https://doi.org/10.1016/j.jalz.2017.06.2269

3 Lim, A. S., Kowgier, M., Yu, L., Buchman, A. S. & Bennett, D. A. Sleep Fragmentation and the Risk of Incident Alzheimer's Disease and Cognitive Decline in Older Persons. *Sleep* **36**, 1027-1032 (2013). https://doi.org/10.5665/sleep.2802

4 Liu, H. *et al.* Acute sleep loss decreases CSF-to-blood clearance of Alzheimer's disease biomarkers. *Alzheimers Dement* (2023). https://doi.org/10.1002/alz.12930

5 Sprecher, K. E. *et al.* Poor sleep is associated with CSF biomarkers of amyloid pathology in cognitively normal adults. *Neurology* **89**, 445-453 (2017). https://doi.org/10.1212/WNL.0000000000004171

6 Sprecher, K. E. *et al.* Amyloid burden is associated with self-reported sleep in nondemented late middle-aged adults. *Neurobiol Aging* **36**, 2568-2576 (2015). https://doi.org/10.1016/j.neurobiolaging.2015.05.004

7 Spira, A. P. *et al.* Self-reported sleep and β-amyloid deposition in community-dwelling older adults. *JAMA Neurol* **70**, 1537-1543 (2013). https://doi.org/10.1001/jamaneurol.2013.4258

8 Winer, J. R. *et al.* Association of Short and Long Sleep Duration With Amyloid-β Burden and Cognition in Aging. *JAMA Neurol* **78**, 1187-1196 (2021). https://doi.org/10.1001/jamaneurol.2021.2876

9 Insel, P. S., Mohlenhoff, B. S., Neylan, T. C., Krystal, A. D. & Mackin, R. S. Association of Sleep and β-Amyloid Pathology Among Older Cognitively Unimpaired Adults. *JAMA Netw Open* **4**, e2117573 (2021). https://doi.org/10.1001/jamanetworkopen.2021.17573

10 Iliff, J. J. *et al.* A paravascular pathway facilitates CSF flow through the brain parenchyma and the clearance of interstitial solutes, including amyloid β. *Sci Transl Med* **4**, 147ra111 (2012). https://doi.org/10.1126/scitranslmed.3003748

11 Iliff, J. J. *et al.* Brain-wide pathway for waste clearance captured by contrast-enhanced MRI. *J Clin Invest* **123**, 1299-1309 (2013). https://doi.org/10.1172/JCI67677

12 Iliff, J. J. *et al.* Cerebral arterial pulsation drives paravascular CSF-interstitial fluid exchange in the murine brain. *J Neurosci* **33**, 18190-18199 (2013). https://doi.org/10.1523/JNEUROSCI.1592-13.2013

13 Xie, L. *et al.* Sleep drives metabolite clearance from the adult brain. *Science* **342**, 373-377 (2013). https://doi.org/10.1126/science.1241224

14 Ringstad, G., Vatnehol, S. A. S. & Eide, P. K. Glymphatic MRI in idiopathic normal pressure hydrocephalus. *Brain* **140**, 2691-2705 (2017). https://doi.org/10.1093/brain/awx191

15 Eide, P. K., Vinje, V., Pripp, A. H., Mardal, K. A. & Ringstad, G. Sleep deprivation impairs molecular clearance from the human brain. *Brain* **144**, 863-874 (2021). https://doi.org/10.1093/brain/awaa443

16 Blennow, K. *et al.* The potential clinical value of plasma biomarkers in Alzheimer's disease. *Alzheimers Dement* **19**, 5805-5816 (2023). https://doi.org/10.1002/alz.13455

17 Rissman, R. A. *et al.* Plasma Aβ42/Aβ40 and phospho-tau217 concentration ratios increase the accuracy of amyloid PET classification in preclinical Alzheimer's disease. *Alzheimers Dement* **20**, 1214-1224 (2024). https://doi.org/10.1002/alz.13542

18 Benedict, C., Blennow, K., Zetterberg, H. & Cedernaes, J. Effects of acute sleep loss on diurnal plasma dynamics of CNS health biomarkers in young men. *Neurology* **94**, e1181-e1189 (2020). https://doi.org/10.1212/WNL.0000000000008866

19 Hablitz, L. M. *et al.* Increased glymphatic influx is correlated with high EEG delta power and low heart rate in mice under anesthesia. *Sci Adv* **5**, eaav5447 (2019). https://doi.org/10.1126/sciadv.aav5447

20 Jiang-Xie, L. F. *et al.* Neuronal dynamics direct cerebrospinal fluid perfusion and brain clearance. *Nature* **627**, 157-164 (2024). https://doi.org/10.1038/s41586-024-07108-6

21 Dagum, P. *et al.* The use of continuous brain parenchymal impedance dispersion to measure glymphatic function in humans. *medRxiv* (2024). https://doi.org/10.1101/2024.01.06.24300933

22 Elbert, D. L., Patterson, B. W., Lucey, B. P., Benzinger, T. L. S. & Bateman, R. J. Importance of CSF-based Aβ clearance with age in humans increases with declining efficacy of blood-brain barrier/proteolytic pathways. *Commun Biol* **5**, 98 (2022). https://doi.org/10.1038/s42003-022-03037-0

23 Diagnostics, C. N. <https://c2n.com/> (

24 Meyer, M. R. *et al.* Clinical validation of the PrecivityAD2 blood test: A mass spectrometry-based test with algorithm combining %p-tau217 and Aβ42/40 ratio to identify presence of brain amyloid. *Alzheimers Dement* **20**, 3179-3192 (2024). https://doi.org/10.1002/alz.13764

25 Fogelman, I. *et al.* Independent study demonstrates amyloid probability score accurately indicates amyloid pathology. *Ann Clin Transl Neurol* **10**, 765-778 (2023). https://doi.org/10.1002/acn3.51763

26 Hu, Y. *et al.* Assessment of a Plasma Amyloid Probability Score to Estimate Amyloid Positron Emission Tomography Findings Among Adults With Cognitive Impairment. *JAMA Netw Open* **5**, e228392 (2022). https://doi.org/10.1001/jamanetworkopen.2022.8392

27 Fultz, N. E. *et al.* Coupled electrophysiological, hemodynamic, and cerebrospinal fluid oscillations in human sleep. *Science* **366**, 628-631 (2019). https://doi.org/10.1126/science.aax5440

28 Helakari, H. *et al.* Human NREM Sleep Promotes Brain-Wide Vasomotor and Respiratory Pulsations. *J Neurosci* **42**, 2503-2515 (2022). https://doi.org/10.1523/JNEUROSCI.0934-21.2022

29 Iliff, J. J. *et al.* Impairment of glymphatic pathway function promotes tau pathology after traumatic brain injury. *J Neurosci* **34**, 16180-16193 (2014). https://doi.org/10.1523/JNEUROSCI.3020-14.2014

30 Harrison, I. F. *et al.* Impaired glymphatic function and clearance of tau in an Alzheimer's disease model. *Brain* **143**, 2576-2593 (2020). https://doi.org/10.1093/brain/awaa179

31 Ishida, K. *et al.* Glymphatic system clears extracellular tau and protects from tau aggregation and neurodegeneration. *J Exp Med* **219** (2022). https://doi.org/10.1084/jem.20211275

32 Orduña Dolado, A. *et al.* Effects of time of the day at sampling on CSF and plasma levels of Alzheimer' disease biomarkers. *Alzheimers Res Ther* **16**, 132 (2024). https://doi.org/10.1186/s13195-024-01503-x

33 Du, L. *et al.* Longitudinal plasma phosphorylated-tau217 and other related biomarkers in a non-demented Alzheimer's risk-enhanced sample. *Alzheimers Dement* (2024). https://doi.org/10.1002/alz.14100

34 Barthélemy, N. R. *et al.* Highly accurate blood test for Alzheimer's disease is similar or superior to clinical cerebrospinal fluid tests. *Nat Med* **30**, 1085-1095 (2024). https://doi.org/10.1038/s41591-024-02869-z

35 Park, H., Tarpey, T., Petkova, E. & Ogden, R. T. A high-dimensional single-index regression for interactions between treatment and covariates. *Statistical Papers* (2024). https://doi.org/10.1007/s00362-024-01546-0

36 West, T. *et al.* A blood-based diagnostic test incorporating plasma Aβ42/40 ratio, ApoE proteotype, and age accurately identifies brain amyloid status: findings from a multi cohort validity analysis. *Mol Neurodegener* **16**, 30 (2021). https://doi.org/10.1186/s13024-021-00451-6

37 Jack, C. R. *et al.* NIA-AA Research Framework: Toward a biological definition of Alzheimer's disease. *Alzheimers Dement* **14**, 535-562 (2018). https://doi.org/10.1016/j.jalz.2018.02.018

38 Biel, D. *et al.* Tau-PET and in vivo Braak-staging as prognostic markers of future cognitive decline in cognitively normal to demented individuals. *Alzheimers Res Ther* **13**, 137 (2021). https://doi.org/10.1186/s13195-021-00880-x

39 Jack, C. R. *et al.* Revised criteria for diagnosis and staging of Alzheimer's disease: Alzheimer's Association Workgroup. *Alzheimers Dement* (2024). https://doi.org/10.1002/alz.13859

40 van Dyck, C. H. *et al.* Lecanemab in Early Alzheimer's Disease. *N Engl J Med* **388**, 9-21 (2023). https://doi.org/10.1056/NEJMoa2212948

41 Sims, J. R. *et al.* Donanemab in Early Symptomatic Alzheimer Disease: The TRAILBLAZER-ALZ 2 Randomized Clinical Trial. *JAMA* **330**, 512-527 (2023). https://doi.org/10.1001/jama.2023.13239

42 Mestre, H. *et al.* Aquaporin-4-dependent glymphatic solute transport in the rodent brain. *Elife* **7** (2018). https://doi.org/10.7554/eLife.40070

43 Pedersen, T. J., Keil, S. A., Han, W., Wang, M. X. & Iliff, J. J. The effect of aquaporin-4 mis-localization on Aβ deposition in mice. *Neurobiol Dis* **181**, 106100 (2023). https://doi.org/10.1016/j.nbd.2023.106100

44 Simon, M. *et al.* Loss of perivascular aquaporin-4 localization impairs glymphatic exchange and promotes amyloid β plaque formation in mice. *Alzheimers Res Ther* **14**, 59 (2022). https://doi.org/10.1186/s13195-022-00999-5

45 Xu, Z. *et al.* Deletion of aquaporin-4 in APP/PS1 mice exacerbates brain Aβ accumulation and memory deficits. *Mol Neurodegener* **10**, 58 (2015). https://doi.org/10.1186/s13024-015-0056-1

46 Kress, B. T. *et al.* Impairment of paravascular clearance pathways in the aging brain. *Ann Neurol* **76**, 845-861 (2014). https://doi.org/10.1002/ana.24271

47 Li, M. *et al.* Impaired Glymphatic Function and Pulsation Alterations in a Mouse Model of Vascular Cognitive Impairment. *Front Aging Neurosci* **13**, 788519 (2021). https://doi.org/10.3389/fnagi.2021.788519

48 Wang, M. *et al.* Focal Solute Trapping and Global Glymphatic Pathway Impairment in a Murine Model of Multiple Microinfarcts. *J Neurosci* **37**, 2870-2877 (2017). https://doi.org/10.1523/JNEUROSCI.2112-16.2017

49 Braun, M. *et al.* Macroscopic changes in aquaporin-4 underlie blast traumatic brain injury-related impairment in glymphatic function. *Brain* **147**, 2214-2229 (2024). https://doi.org/10.1093/brain/awae065

50 Christensen, J., Wright, D. K., Yamakawa, G. R., Shultz, S. R. & Mychasiuk, R. Repetitive Mild Traumatic Brain Injury Alters Glymphatic Clearance Rates in Limbic Structures of Adolescent Female Rats. *Sci Rep* **10**, 6254 (2020). https://doi.org/10.1038/s41598-020-63022-7

51 Plog, B. A. *et al.* Biomarkers of traumatic injury are transported from brain to blood via the glymphatic system. *J Neurosci* **35**, 518-526 (2015). https://doi.org/10.1523/JNEUROSCI.3742-14.2015

52 Deng, S. *et al.* Chronic sleep fragmentation impairs brain interstitial clearance in young wildtype mice. *J Cereb Blood Flow Metab*, 271678X241230188 (2024). https://doi.org/10.1177/0271678X241230188

53 Nedergaard, M. & Goldman, S. A. Glymphatic failure as a final common pathway to dementia. *Science* **370**, 50-56 (2020). https://doi.org/10.1126/science.abb8739

54 Eide, P. K. & Ringstad, G. Functional analysis of the human perivascular subarachnoid space. *Nat Commun* **15**, 2001 (2024). https://doi.org/10.1038/s41467-024-46329-1

55 Barthélemy, N. R. *et al.* Sleep Deprivation Affects Tau Phosphorylation in Human Cerebrospinal Fluid. *Ann Neurol* **87**, 700-709 (2020). https://doi.org/10.1002/ana.25702

56 Holth, J. K. *et al.* The sleep-wake cycle regulates brain interstitial fluid tau in mice and CSF tau in humans. *Science* **363**, 880-884 (2019). https://doi.org/10.1126/science.aav2546

57 Tobler, I. & Borbély, A. A. Sleep EEG in the rat as a function of prior waking. *Electroencephalogr Clin Neurophysiol* **64**, 74-76 (1986). https://doi.org/10.1016/0013-4694(86)90044-1

58 Burnham, K. P. & Anderson, D. R. Multimodel Inference: Understanding AIC and BIC in Model Selection. *Sociological Methods & Research* **33**, 261-304 (2004).

59 Brum, W. S. *et al.* Biological variation estimates of Alzheimer's disease plasma biomarkers in healthy individuals. *Alzheimers Dement* **20**, 1284-1297 (2024). https://doi.org/10.1002/alz.13518

60 Martínez-Dubarbie, F. *et al.* Influence of Physiological Variables and Comorbidities on Plasma Aβ40, Aβ42, and p-tau181 Levels in Cognitively Unimpaired Individuals. *Int J Mol Sci* **25** (2024). https://doi.org/10.3390/ijms25031481

61 Pichet Binette, A. *et al.* Confounding factors of Alzheimer's disease plasma biomarkers and their impact on clinical performance. *Alzheimers Dement* **19**, 1403-1414 (2023). https://doi.org/10.1002/alz.12787

62 Kronmal, R. A. Spurious Correlation and the Fallacy of the Ratio Standard Revisited. *Journal of the Royal Statistical Society. Series A (Statistics in Society),* **156**, 379-392 (1993).

63 Berridge, D. M. & Crouchley, R. *Multivariate Generalized Linear Mixed Models Using R*. (CRC Press, 2011).

64 Heinze, G., Wallisch, C. & Dunkler, D. Variable selection - A review and recommendations for the practicing statistician. *Biom J* **60**, 431-449 (2018). https://doi.org/10.1002/bimj.201700067

65 Xu, R. Measuring explained variation in linear mixed effects models. *Stat Med* **22**, 3527-3541 (2003). https://doi.org/10.1002/sim.1572